

# Deliverable D49 (D6.4)

## European added value of implementing the RI-URBANS strategy



**Research Infrastructures Services Reinforcing Air  
Quality Monitoring Capacities in European Urban &  
Industrial Areas (GA n. 101036245)**

**By  
CSIC & UHEL**



***17 September 2025***

## Deliverable D49 (D6.4): European added value of implementing the RI-URBANS strategy

Authors: Xavier Querol (CSIC), Tuukka Petäjä (UHEL)

<b>Work package (WP)</b>	WP6, Stakeholder engagement strategies
<b>Deliverable</b>	D49 (D6.4)
<b>Lead beneficiary</b>	CSIC
<b>Deliverable type</b>	<input checked="" type="checkbox"/> R (document, report) <input type="checkbox"/> DEC (websites, patent filings, videos,...) <input type="checkbox"/> Other: ORDP (open research data pilot)
<b>Dissemination level</b>	<input checked="" type="checkbox"/> PU (public) <input type="checkbox"/> CO (confidential, only members of consortium and European Commission)
<b>Estimated delivery deadline</b>	M48 (30/09/2025)
<b>Actual delivery deadline</b>	17/09/2025
<b>Version</b>	Final
<b>Reviewed by</b>	WP6 leaders and the project coordinators
<b>Accepted by</b>	Project coordination team
<b>Comments</b>	<p>This report summarises the European added value of implanting the results from RI-URBANS. The added value of implementing the service tools delivered by the project is presented at three levels:</p> <p>i) supporting implementation of Art 10 of the Ambient Air Quality Directive (EU) 2024/2881; and</p> <p>ii) supporting implementation of advanced air quality assessments; and ii) examples of results obtained at a European scale.</p>

## Table of Contents

<b>1. ABOUT THIS DOCUMENT.....</b>	<b>1</b>
<b>2. ADDED VALUE IN SUPPORT OF THE IMPLEMENTATION OF THE NAQD.....</b>	<b>2</b>
<b>3. SUPPORTING IMPLEMENTATION OF ADVANCED AQ ASSESSMENT TOOLS.....</b>	<b>5</b>
<b>4. EXAMPLES OF THE EUROPEAN ADDED VALUE OF THE IMPLEMENTATION OF THE STS.....</b>	<b>6</b>
4.1.    ADDED VALUE OF UFP AND PNSD MEASUREMENTS.....	6
4.2.1. <i>Emission inventories of UFP and PNSD</i> .....	10
4.1.2. <i>Modelling of UFP and PNSD</i> .....	12
4.1.3. <i>Specific challenges in UFP and PNSD</i> .....	13
4.2.    ADDED VALUE OF MEASURING EBC CONCENTRATION IN EUROPE.....	13
4.3.    PM SPECIATION AND SOURCE APPORTIONMENT IN URBAN EUROPE USING OFF-LINE PM MEASUREMENTS .....	16
4.3.1. <i>Off-line PM speciation</i> .....	16
4.3.2. <i>Non-refractory PM1 speciation and source apportionment in urban Europe using on-line PM measurements</i> .....	20
<b>4.4.    ADDED VALUE OF MEASURING OXIDATIVE POTENTIAL OF PM IN URBAN EUROPE .....</b>	<b>23</b>
4.5.    THE ADDED VALUE OF MEASURING NH <sub>3</sub> IN URBAN EUROPE .....	25
4.6.    THE ADDED VALUE OF MEASURING VOCs IN URBAN EUROPE.....	29
4.6.1. <i>Emissions of VOCs</i> .....	30
4.6.2. <i>Concentrations of VOCs</i> .....	31
4.6.3. <i>Source apportionment studies of volatile organic compounds in Europe</i> .....	33
<b>4.7.    ADDED VALUE OF MEASURING VERTICAL PROFILES .....</b>	<b>35</b>
4.7.1. <i>Atmospheric boundary layer</i> .....	35
4.7.2. <i>Vertical profiles of aerosols</i> .....	36
4.7.3. <i>IAGOS vertical profiles of pollutants</i> .....	38
4.8.    ADDED VALUES OF URBAN MAPPING AND CITIZEN SCIENCE .....	40
4.8.1. <i>Mapping of novel AQ parameters</i> .....	40
4.8.2. <i>Mapping and involvement of citizen science</i> .....	42
<b>5.    FINAL CONSIDERATIONS.....</b>	<b>43</b>

## 1. About this document

This document is delivered in the framework of the RI-URBANS project (Research Infrastructure Services for Strengthening Air Quality (AQ) Monitoring Capacities in European Urban and Industrial AreaS), which aims to expand and adapt atmospheric Research Infrastructure (RI) services to enhance AQ observations in support of advanced policy assessment. The project seeks to build, develop, and foster synergies between Air Quality Monitoring Networks (AQMNs) and atmospheric RIs to improve the capacity of AQMNs to provide the observations needed to assess, forecast, and reduce urban air pollution. Pilot Service Tools (STs) combining advanced scientific knowledge and innovative technical work have been developed to this end and offered to AQMNs to support AQ observations and better address challenges and social demands associated with AQ in European cities and industrial hotspots.

In RI-URBANS, STs are any tools that the project helped to review, in some cases develop, test, and ultimately recommend for advanced AQ assessment in urban areas. Such tools support AQ assessment in accordance with RI-URBANS AQ monitoring and modelling recommendations for novel pollutants. These include protocols for measuring advanced AQ variables (derived from ACTRIS and CEN or, in specific cases, proposed when not available), mapping protocols, emission inventories, modelling tools, and suggested epidemiological approaches to evaluate the health effects of new pollutants.

WP6 aims at maximising engagement of stakeholders to ensure the transfer and implementation of RI-URBANS' STs and the demonstration of the project's societal and environmental benefits, by implementing suitable strategies to engage different groups of AQ stakeholders, with a focus on enhancing the AQMNs-RIs links.

The specific objectives:

- Maximise involvement of local, regional and national administrations for selecting novel AQ metrics, implementing and interpreting pilot studies, and being receptors of the deliverables and reports.
- Providing guidance for engaging citizens for measurements and increasing awareness on the novel AQ metrics.
- Involving European administrations and AQ and AQ-Health agencies, such as EMEP-UNECE, EEA, WHO, and Copernicus along the process to communicate progress, participate in the discussions and workshops, and visit them to communicate the outputs.

Because the review of the new Ambient Air Quality Directive (NAQD) was launched on 26th October 2022 and in its draft proposal it was included creating a network of AQ supersites for the measurement of the advanced parameters included in RI-URBANS, we considered very relevant to enhance an objective for WP6, which is part of iii): Supply technical guidance to Directorate General of Environment (DG-ENV) from the European Commission (EC) and the Network of European AQ National Reference Laboratories (AQUILA) to support implementation of measurements of the advanced AQ parameters included in the NAQD, 2024/2881, from 10<sup>th</sup> December 2024.

Sixteen STs were developed and are now available to support optimised urban AQ management. For each STs, a specific guidance document illustrates the tool in detail and supports the uptake and suitable

implementation of these measurements and modelling by relevant stakeholders, such as AQ authorities, networks, and scientists. The STs documents are reported in the project deliverable [D46 \(D6.1\) - Information packages for local, regional and national AQ administrations](#), and offer actionable recommendations and guidance on measurements, source apportionment (SA), health assessment, mapping, and modelling.

A [booklet](#) was produced to support the dissemination and the in situ presentation of the STs and the related information package, also highlighting their added value for measuring advanced AQ variables for enhanced AQ assessment. The elaboration of these 17 documents made up [D46 \(D6.1\)](#) and [D56 \(D7.6\)](#).

This document, D49 (D6.4) summarises the European added value of implanting the results from RI-URBANS. The added value of implementing the STs delivered by the project is presented at three levels: i) supporting implementation of Art 10 of the new Ambient AQ Directive (EU) 2024/2881 (NAQD); ii) supporting implementation of advanced AQ assessment tools; and iii) examples of results obtained at a European scale.

This is a public document that will be distributed to all RI-URBANS partners for their use and submitted to the European Commission as the RI-URBANS deliverable D49 (D6.4) This document can be downloaded at <https://riurbans.eu/work-package-6/#deliverables-wp6>

## **2. Added value in support of the implementation of the NAQD**

From the beginning of the RI-URBANS project we interacted with key stakeholders to favour the co-design of the STs and data management. The results were very relevant in such a way that some of the new AQ parameters suggested by RI-URBANS were included in the NAQD, and the key RI-URBANS' STs guidance documents are cited frequently in the official guidance for AQ measurements produced by DG-ENV. The first added values of implementing the results of RI-URBAN are (Figure 2.1):

- In the [base documents of the first draft of the NAQD](#), RI-URBANS was mentioned (inside ACTRIS) as a source of information for new air pollutants and supersites in Art 10.
- [The final DG ENV report on monitoring](#) to support the implementations of the NAQD was made publicly available on May 2025, and contains 29 references to RI-URBANS STs for recommending implementing the measurements of Article 10 of the NAQD. Special relevance is given to RI-URBANS guidance documents on measurements of ultrafine particles (UFP), particle number size distribution (PNSD), Black Carbon BC), atmospheric particulate matter (PM) speciation, ammonia (NH<sub>3</sub>), oxidative potential (OP), and volatile organic compounds (VOCs). Thus, all AQMNs will have access to RI-URBANS guidance documents for STs through this official document. Also 2 references to RI-URBANS STs are included in the [twin DG report on modelling](#).

The reasons why RI-URBANS suggested supersites measuring UFP-PNSD, BC, PM speciation, OP, VOCs and NH<sub>3</sub> are summarised below:

- **ST1:** The White Paper on ambient **UFP:** Evidences for policy for makers ([Casseo et al., 2019](#)) reviewed studies on exposure to UFP and associated health effects and concluded that there is still an inconsistency of results concerning health impact. They attributed this inconsistency to several possibilities, including i) the lack of harmonised measurement protocols; ii) the use of a single site to evaluate health effects for a whole city; and iii) the variety of sources of UFP that might difficult finding generalised health effect associations. Subsequently,

the World Health Organization (WHO) AQ Guidelines ([WHO, 2021](#)) referred to this White Paper to highlight the above conclusions and suggested to implement harmonised UFP measurements. Even if [WHO \(2021\)](#) did not propose guideline values for UFP, a rank of concentrations was suggested to identify low and high exposure concentrations.

- **ST1 and ST11:** Given that the source contributions of UFP may vary in different cities, RI-URBANS considered that measuring also PNSD will allow performing accurate interpretations of these source contributions, and not only provide relevant results for epidemiological studies, but also evaluating the effect of policy actions and propose new ones.
- **ST2 and ST11:** [WHO \(2012\)](#), and many more recent specific studies) found short-term exposure to BC is associated with all-cause and cardiovascular mortality, and cardiopulmonary hospital admissions. Probably this is not a *per se* effect of BC (graphitic C) but most probably caused by substances transported by BC,-rich aerosols, such as Polycyclic Aromatic Hydrocarbons (PAHs). Furthermore, for policy information BC is a good tracer of road traffic and biomass/coal burning contributions, and it is also relevant to evaluate impacts of policy measures and to suggest new ones.

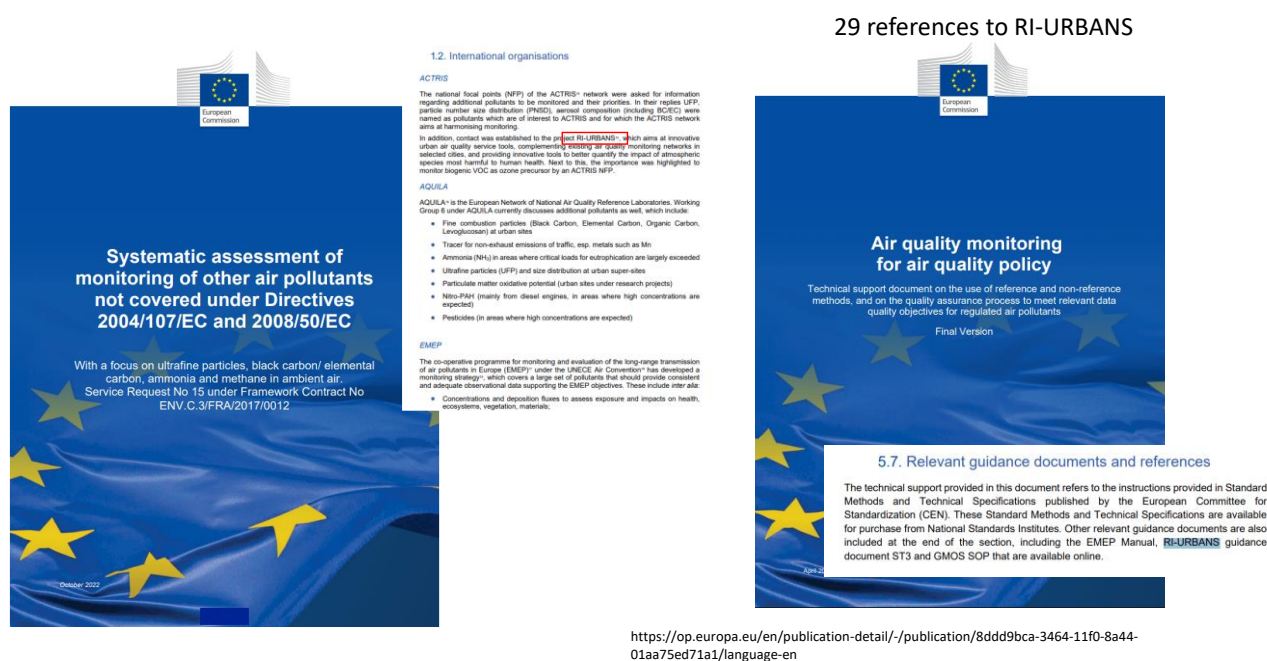


Figure 2.1. Demonstration of the Impact of RI-URBANS impact in the NAQD elaboration and implementation.



Figure 2.2. Two relevant policy oriented documents suggesting measurements of UFP, and one of them also BC.

- **ST3 and ST10:** A detailed PM speciation characterisation may provide very relevant information for identifying the main PM components causing the different known health effects, if these monitoring data are used in epidemiological data. Furthermore, these data may provide the basis to implement receptor modelling for SA, highly valuable data for epidemiological studies and policy assessment. Furthermore, include additional metals (to As, Cd, Ni, and Pb) required by AQ standards does not increase dramatically monitoring costs. The PM speciation data suggested to include both offline and online methods, the latter supporting near-real-time (NRT) policy decisions for AQ.
- **ST4, ST10, ST11:** OP was considered relevant because this is a good tracer of toxicity caused oxidative stress, mostly associated to respiratory air pollution derived outcomes. However, as for UFP-PNSD, OP is measured by different protocols, and there is a need for a harmonised protocol to compare different studies. Furthermore, OP combined with PM speciation (ST3) and source apportionment (ST10 and ST11) allow to identify PM components and sources causing OP. To this end a simplified OP measurement protocol for OPDTT and another for OPAA have been proposed by RI-URBANS.
- **ST5 & ST11:** VOCs species are precursors of ozone (O<sub>3</sub>) and the main component of PM<sub>2.5</sub>, secondary organic aerosols (SOA). To abate PM and O<sub>3</sub> concentrations it is key having information on the VOCs speciation and the SA. ST5 covers the guidance for VOCs measurements and ST11 the SA approaches.
- **ST6:** In the NAQD, measurements of NH<sub>3</sub> are requested for rural supersites, but not for the urban ones, where this is only recommended. However, in the urban pollution hotspots, NH<sub>3</sub> measurements are very relevant to evaluate possible effects of AQ policy actions to abate fine particulate matter (PM<sub>2.5</sub>), since this pollutant has a key role in the generation of secondary inorganic PM (the second major component of PM<sub>2.5</sub>).
- **ST7, 8 & 9:** contribution of natural emissions to PM<sub>2.5</sub> and PM<sub>10</sub> mass concentrations at the ground level is influenced by long-range transport of dust. STs 7-9 provide guidance for harmonized vertical profiling of the boundary layer and quantification of elevated aerosol layers, which will enable differentiating the anthropogenic and natural contribution of PM mass concentrations since the natural contribution can be excluded from the number of mass concentration exceedances.

The NAQD includes the above novel AQ parameters. We do not know if this is a coincidence or that the first draft of the NAQD considered the information sent in October 2021 to the team writing the base documents of the draft.

Furthermore, the interaction with subsequent teams involved in the writing of documents for the implementation of the NAQD prompted in a high impact of the STs1-6 RI-URBANS' guidance documents, which are cited 29 times in the [official document supporting the implementations of measurements in the NAQD](#).

Another key indicator of the added value of the RI-URBANS' contribution to the implementation of the NAQD is that DG-ENV invited RI-URBANS, with a stand, to be present in the 2025 Air Quality Forum in December 2025.

### **3. Supporting implementation of advanced AQ assessment tools**

There are a number of STs that were not included in the NAQD, but RI-URBANS propose them to build up an advanced AQ assessment to support the difficult compliance of the 2030 limit values and target values of the NAQD.

**ST7:** Currently, most AQMNs miss information about important processes and quantities in the vertical dimension that are necessary to better understand surface-level pollution data. The vertical dimension is especially relevant when considering potential non-local sources of aerosols (e.g. those arriving via medium-to-long-range transport) or for evaluating vertical dilution of locally emitted pollutants (for example, to forecast exceedances of specific daily limit values), among others. This RI-URBANS/ACTRIS guidance document highlights the added value provided by information from measurements of **atmospheric boundary layer** height and dynamics. The main instruments allowing these measurements are briefly outlined, as well as the operation requirements. The document presents a few selected examples of measurements and retrievals that are applied in different RI-URBANS pilot cities and beyond.

**ST8:** Similarly, to ST7, this RI-URBANS/ACTRIS guidance document focuses on the added value of vertical measurements. The aim of this document is to facilitate the consideration of **aerosol profiling** within AQMNs. A concise summary of the currently available methodologies is provided, focusing on very precise methods, as well as a synthesis of Pan-European observations. These are specially valuable to demonstrate the long-range transport and natural contributions to PM.

**ST9:** RI-URBANS connects the atmospheric observation expertise from IAGOS to the urban AQ. This guidance document describes the available AQ parameters from IAGOS profiling, the data access, and examples of the use of **IAGOS profiles** over RI-URBANS pilot cities.

**ST12:** This RI-URBANS guidance document focuses on the application of **deterministic modelling for mapping PM and UFP at urban scale**. Pollutants such as NO<sub>2</sub>, PM<sub>2.5</sub>, BC and UFP may strongly impact the health of the population, with their concentrations being often particularly high over cities, with strong urban heterogeneities. In cities, concentration of NO<sub>2</sub>, BC and particle number (PN) and to a lesser extent PM<sub>2.5</sub> are particularly high along traffic axes and in streets. To estimate the outdoor concentration exposure of the population, maps are required at spatial scales finer than 100 m, at the minimum, to be able to differentiate the street from the urban background concentrations. Hourly time resolution is desirable.

**ST13:** This RI-URBANS guidance document describes methods that AQMNs, researchers and other groups can use to develop **fine spatial resolution maps of urban air pollution derived from monitoring**. The methods described in this document are complementary to routine monitoring with reference equipment at one or a few monitoring sites across the city. The described methods are also complementary to deterministic dispersion models which are often applied by AQ agencies for regulatory purposes. The methods for involvement of citizen science for such mappings are also reviewed.

**ST14:** This RI-URBANS guidance document focuses on **the steps needed to conduct an epidemiological analysis linking novel AQ pollutants** with health effects. Estimates of short-term associations between air pollution and health are usually based on studying the relationship between daily variations of air pollutant concentrations and daily counts of health outcomes such as mortality and/or morbidity (e.g. hospital admissions or hospital visits by various causes). This document reports on the different options that can be followed to conduct epidemiological studies, the data needs and the statistical methodologies that can be applied. Lastly, it illustrates, using the data compiled by the RI-URBANS project, the feasibility of implementing such analyses and the added value of the novel AQ pollutants to determine health effects.

**ST15:** This RI-URBANS guidance document focuses on the steps needed to produce **consistent emission inventories for regional and urban scale modelling** applications. It describes the specific improvements that have been made to existing European emission inventories for RI-URBANS at a horizontal resolution of ~6x6 km<sup>2</sup> to better represent road transport emissions and include estimations of UFP, among others. This document also describes a downscaling tool to detail the European emission dataset to a 1x1 km<sup>2</sup> resolution over urban areas in a consistent way. The specific **RI-URBANS emission inventories are elaborated for: UFP-PNSD, non-exhaust PM, other anthropogenic sources of PM and its components, including BC, and NO<sub>x</sub>, SO<sub>x</sub> (sulphur oxides), NH<sub>3</sub> and VOCs.** The European wide emission inventories can be obtained directly through access to an FTP repository, or by requesting these via email ([Jeroen.Kuenen@tno.nl](mailto:Jeroen.Kuenen@tno.nl) or [Marya.ElMalki@tno.nl](mailto:Marya.ElMalki@tno.nl)), while urban (1x1 km<sup>2</sup>) emission datasets for cities of Amsterdam, Athens, Birmingham and Helsinki can be obtained by the same FTP repository or by requesting them via email ([eathana@noa.gr](mailto:eathana@noa.gr)).

**ST16:** This RI-URBANS guidance document focuses on guidance to **adequately model the spatial-temporal variation of UFP and PNSD.** To this end, primary UFP-PNSD emission inventories are required (see [ST15](#) on the first UFP-PNSD EU emission inventory), but also complex physical-chemical processes for nucleation should be implemented in the modelling tools. Multiscale approaches are required to account for emission and particle formation if the urban UFP-PNSD are intended to be modelled. This document summarises methodologies for multiscale modelling of UFP using two approaches, PMCAMx-UF (a three-dimensional chemical transport model focusing on the simulation of the UFP-PNSD and composition; Jung et al., 2010) and CHIMERE (a multi-scale chemistry-transport model for atmospheric composition analysis and forecast).

All the STs summarised above have been developed and reviewed by a large group of experts in the field of AQ management and research; and many of these co-designed with EU stakeholders. These STs have been produced RI-URBANS by experts from WPs 1-3, but also from WP4 by including results of the pilot testing of the STs. WP6 compiled the information and yield to the 17 Guidance documents.

## **4. Examples of the European added value of the implementation of the STs**

### **4.1. Added value of UFP and PNSD measurements**

It is widely recognised that exposure to PM negatively impacts human health (WHO, 2021). Several studies have also shown that UFP can penetrate deeply into the respiratory system, thus causing respiratory and cardiovascular diseases in humans ([Cassee et al., 2019](#), and references therein). In the range <10 nm, a rapidly increasing fraction of particles are lost by diffusion in the nose, oral cavity, and trachea. The sizes of UFPs not only allow them to reach the deeper parts of the respiratory system, but a fraction of these can reach the alveoli, translocate and reach the circulatory system, and, from there, they can reach any organ in the body, or directly reach the brain by translocating the olfactory bulb of the brain ([Cassee et al., 2019](#), and references therein). The new WHO AQ Guidelines ([WHO, 2021](#)) identify UFP concentration as a relevant AQ parameter and find that, although there is a

body of evidence for the health effects of UFPs, results are still inconsistent. [Cassee et al. \(2019\)](#) and [Rivas et al. \(2021\)](#) reported that this inconsistency may be, at least in part, due to methodological differences in measurements, to the lack of representation of human exposure to UFPs resulting from the use of only a single monitoring station per city in most studies, and the different sources contributing to UFP concentrations in other cities/regions. Although the [WHO \(2021\)](#) does not provide guideline values, the monitoring of concentrations of UFPs and BC is recommended to allow a more accurate evaluation of their health effects. However, [WHO \(2021\)](#) provides a good practice statement, in which they state that low ambient air concentration can be considered to be  $<1000 \text{ \# cm}^{-3}$  and high concentration  $>10000 \text{ \# cm}^{-3}$  as a 24h mean value.

RI-URBANS carried out a compilation and interpretation of 27 long datasets of UFP-PNSDs in urban Europe ([Trechera et al., 2023](#)). The results showed that UFP concentrations are typically higher closer to source areas, such as traffic and industrial hotspots and the concentrations are lower in urban and suburban background areas (Figure 4.1). The diurnal cycle at traffic sites follows anthropogenic traffic and combustion source patterns with a contribution of photochemical production of nanoparticles during daytime. Night-time concentrations are lower due to lower UFP emissions. Typically, UFP concentrations in urban environments are higher during wintertime due to reduced vertical mixing and increased anthropogenic sources.

Focusing on urban background sites the highest annual averaged PNCs were recorded in eastern and southern Europe (11200 to 10300  $\text{\# cm}^{-3}$ ) and two central European sites (close to 10000  $\text{\# cm}^{-3}$ ), followed by central-southern Europe (8900 to 6200  $\text{\# cm}^{-3}$ ) and north and north-western Europe and Switzerland (4500 to 3500  $\text{\# cm}^{-3}$ ) (Figure 4.2).

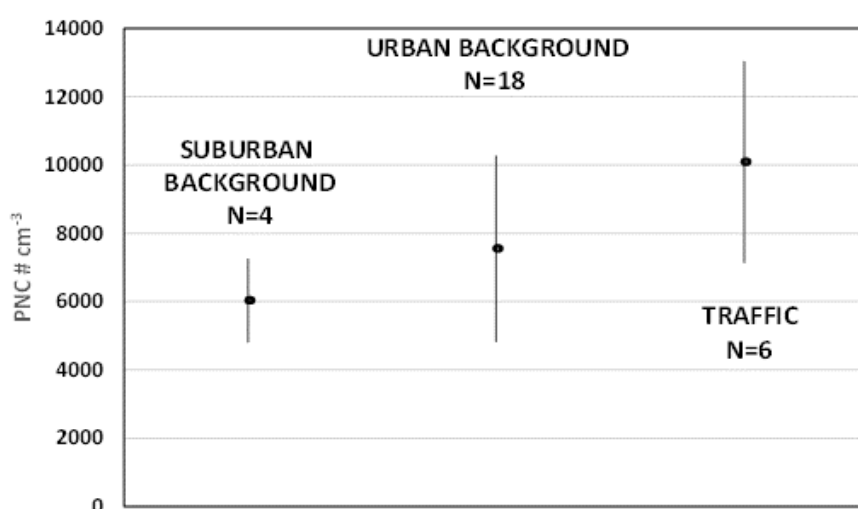


**Figure 4.1.** Average UFP concentrations and standard deviation ranges of suburban and urban background and traffic sites. Data from [Trechera et al. \(2023\)](#).

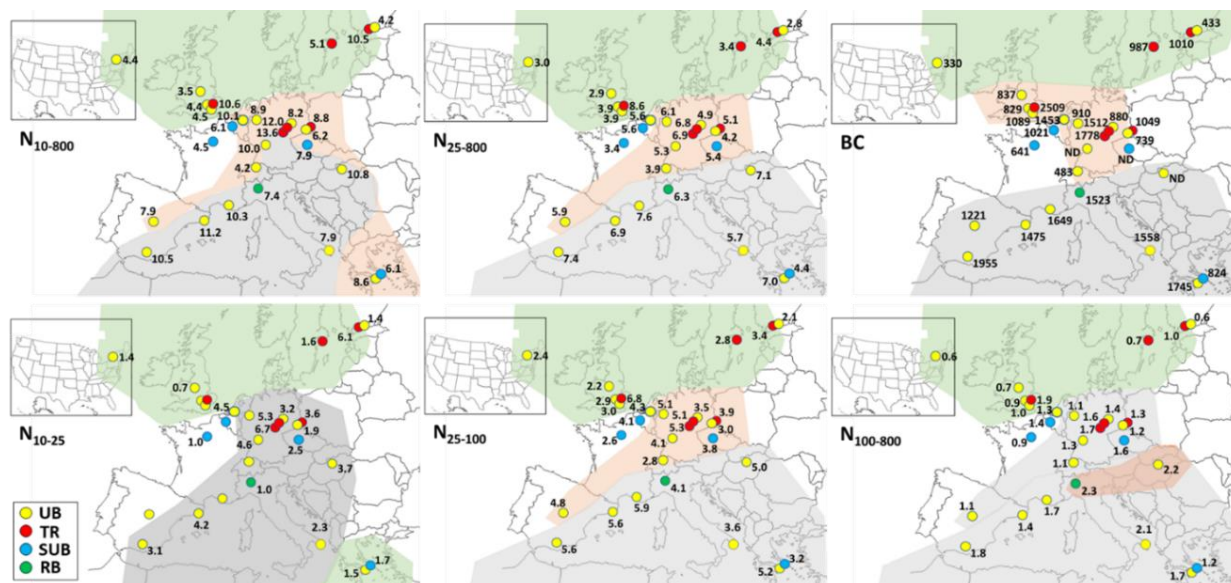


**Figure 4.2.** Regional variability of averaged 2017–2019 particle number concentrations (in  $\# \text{cm}^{-3} 10^3$ ) size fractions (in  $\# \text{cm}^{-3} 10^3$ ) and black carbon (BC in  $\text{ng m}^{-3}$ ) in Europe. For the size fraction of 10–25 nm ( $N_{10-25}$ ), only sites with a lower size detection limit of 10–14 nm are included. UB, Urban background; TR, traffic; SUB, Suburban background; RB, Regional background. Modified from [Trechera et al. \(2023\)](#).

PNSD measurements were used for source contribution analyses of urban UFP. [Garcia-Marlès et al. \(2024a\)](#) summarized the pan-European SA analysis based on PNSD (Figure 4.3). Focusing on European urban background and traffic sites, traffic-related UFP contributions dominate PNC, followed by photochemical nucleation or new particle formation producing particles close to the detection limit of the instrument (10 nm). Shipping and aviation might also contribute to increasing UFP concentrations with a prevalence of the lowest size mode ([Diesch et al., 2013](#); [Lorentz et al., 2019](#); [Stacey et al., 2021](#)). The UFP sources also include biomass burning, urban background sources, industrial emissions, mixed sources, dust and unknown sources ([Hopke et al., 2022](#)).

Long-term data on UFP and PNSD in different European urban environments will allow analysis of trends in the concentrations and PNSD. As shown in [Garcia-Marlès et al. \(2024a, b\)](#), this can be used to quantify impacts of new AQ policies, such as implementation of EURO5/EURO6 engine emission policies, impact of local low-emission zones or quantifying the changes in AQ and air pollution exposure during electrification of the traffic fleet. The long-term UFP and PNSD data can help to identify emerging needs, such as the one of applying controls for semi volatile VOCs (SVOCs) in the diesel filter traps. During the regeneration cycles they emit SVOCs that cause nucleation of UFP very close to the exhaust emissions. The results from [Garcia-Marlès et al. \(2024a, b\)](#) showed that the traffic nucleation source did not have a consistent decreasing trend, while the diesel contribution and Aitken and accumulation modes did (Figure 4.4).

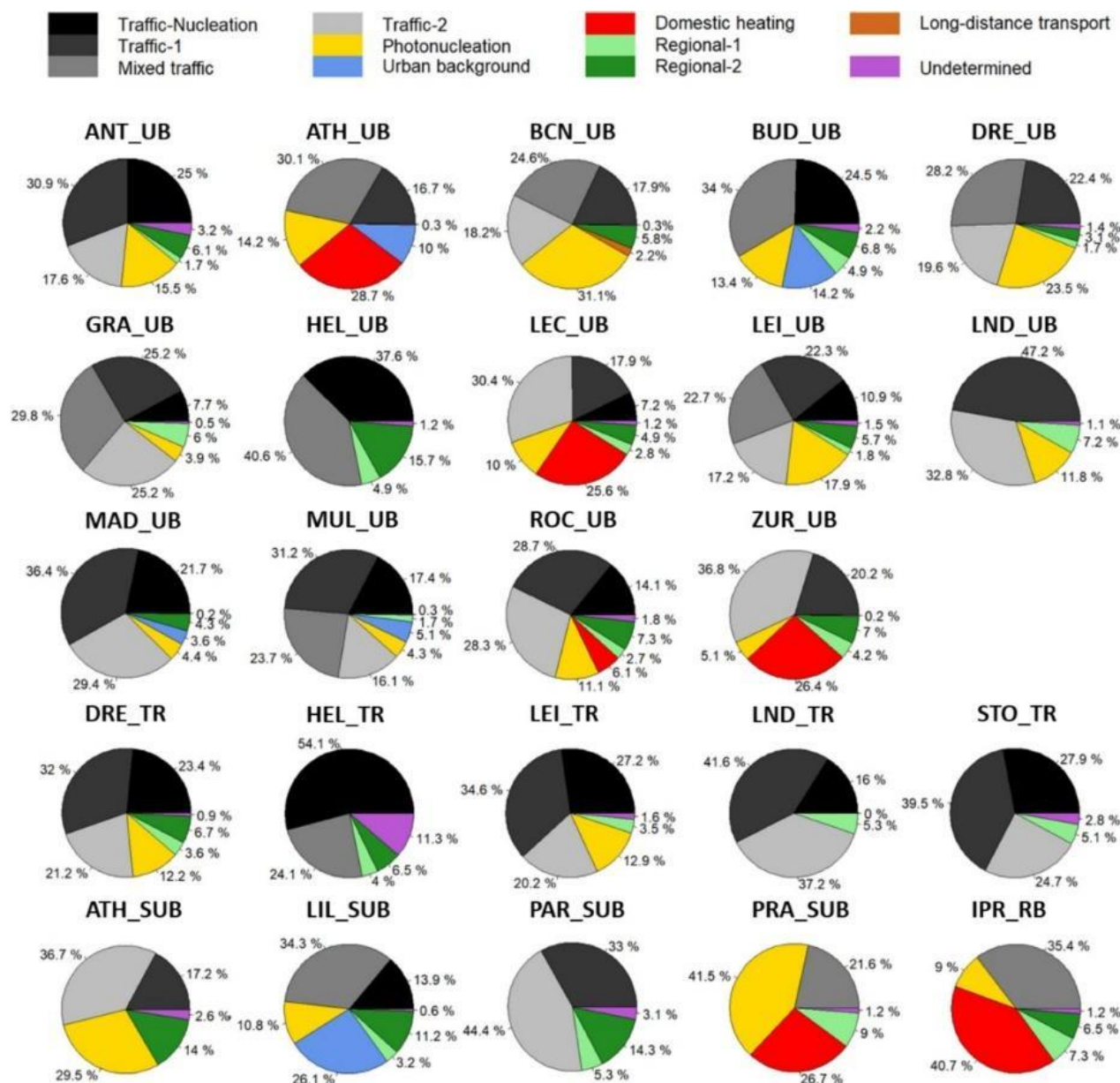


**Figure 4.3.** Results of the source apportionment of PNCs based on PNSD time series from 24 supersites in urban Europe. Figure from [Garcia-Marlès et al. \(2024b\)](#). UB and SUB, urban and suburban background; RB, regional background; TR, traffic sites. Antwerp (ANT\_UB), Athens (ATH\_UB), Barcelona (BCN\_UB), Budapest (BUD\_UB), Dresden (DRE\_UB), Granada (GRA\_UB), Helsinki (HEL\_UB), Lecce (LEC\_UB), Leipzig (LEI\_UB), London (LND\_UB), Madrid (MAD\_UB), Mülheim (MUL\_UB), Zurich (ZUR\_UB), and Rochester (ROC\_UB) in New York State in USA. Dresden (DRE\_TR), Helsinki (HEL\_TR), Leipzig (LEI\_TR), London (LND\_TR) and Stockholm (STO\_TR). Athens (ATH\_SUB), Lille (LIL\_SUB), Paris (PAR\_SUB) and Prague (PRA\_SUB). Ispra (IPR\_RB).

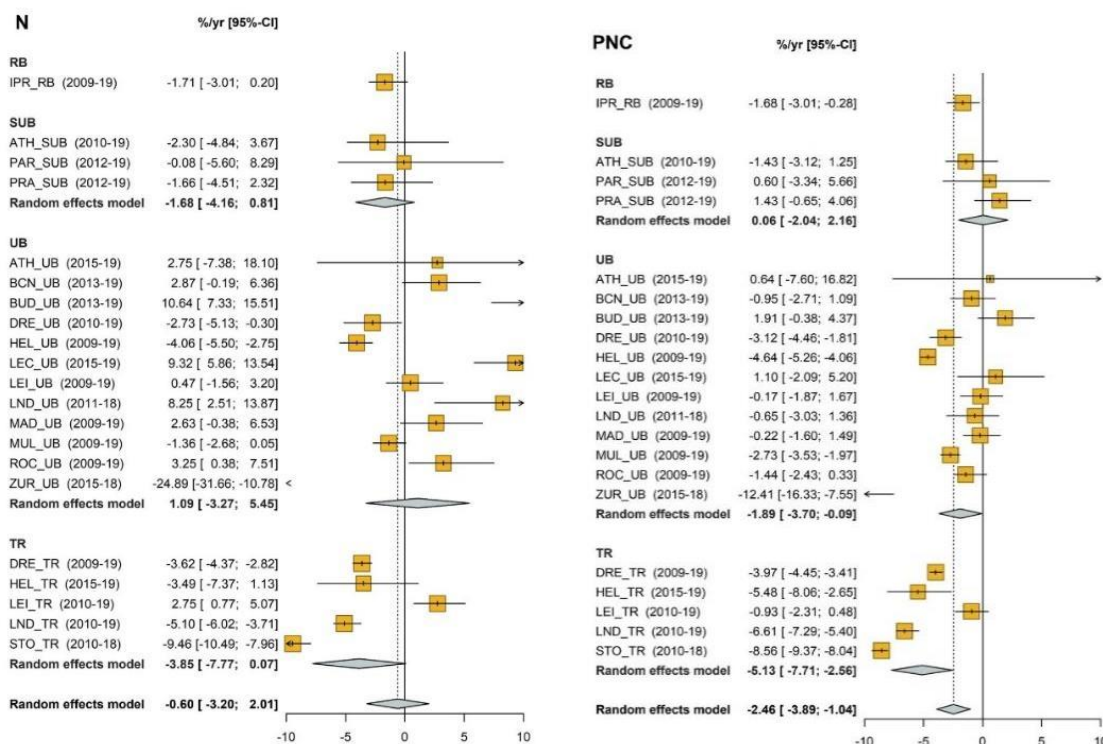


**Figure 4.** Results of the trend analysis and subsequent meta-analysis for Nucleation mode particle concentration (N), and total particle number concentrations (PNC). Trends are calculated using the Theil-Sen method. The dashed lined represents the global meta-analysis. Random effects model is the mean effect calculated for each site type. UB and SUB, urban and suburban background; RB, regional background; TR, traffic sites. Antwerp (ANT\_UB), Athens (ATH\_UB), Barcelona (BCN\_UB), Budapest (BUD\_UB), Dresden (DRE\_UB), Granada (GRA\_UB), Helsinki (HEL\_UB), Ispra (IPR\_RB), Lecce (LEC\_UB), Leipzig (LEI\_UB), London (LND\_UB), Madrid (MAD\_UB), Mülheim (MUL\_UB), Zurich (ZUR\_UB), and Rochester (ROC\_UB) in New York State in USA. Dresden (DRE\_TR), Helsinki (HEL\_TR), Leipzig (LEI\_TR), London (LND\_TR) and Stockholm (STO\_TR). Athens (ATH\_SUB), Lille (LIL\_SUB), Paris (PAR\_SUB) and Prague (PRA\_SUB). Figure from [Garcia-Marlès et al. \(2024a\)](#).

#### 4.2.1. Emission inventories of UFP and PNSD

**ST15** elaborated European wide emission inventories (at a horizontal resolution of  $\sim 6 \times 6 \text{ km}^2$ ) and urban ones ( $1 \times 1 \text{ km}^2$ ) for the urban areas of Amsterdam, Athens, Birmingham and Helsinki for UFP-PNSD, non-exhaust PM, other anthropogenic sources of PM and its components, including BC, and  $\text{NO}_x$ ,  $\text{SO}_x$ ,  $\text{NH}_3$  and VOCs. Figure 4.5 shows as an example the contribution of the different sub-sources in road transport to total emissions in 2019 according to this inventory. It shows that – depending on the pollutant – cold start emissions vary between 3% and 18% of UFP emissions, whereas for  $\text{PM}_{10}$  the non-exhaust accounts for 60% of total emissions, while for  $\text{PM}_{2.5}$  this share is around 45%. For total particle number, TPN (equivalent to UFP) the hot engine emissions reach 95% of TPN from road traffic. Other examples are shown in Figure 4.6, which compares TPN and  $\text{PM}_{2.5}$  emissions for the different sectors, with domestic combustion > energy and industry >> waste and agriculture being the main contributors for  $\text{PM}_{2.5}$  and shipping > road transport > energy and industry >> aviation for TPN.

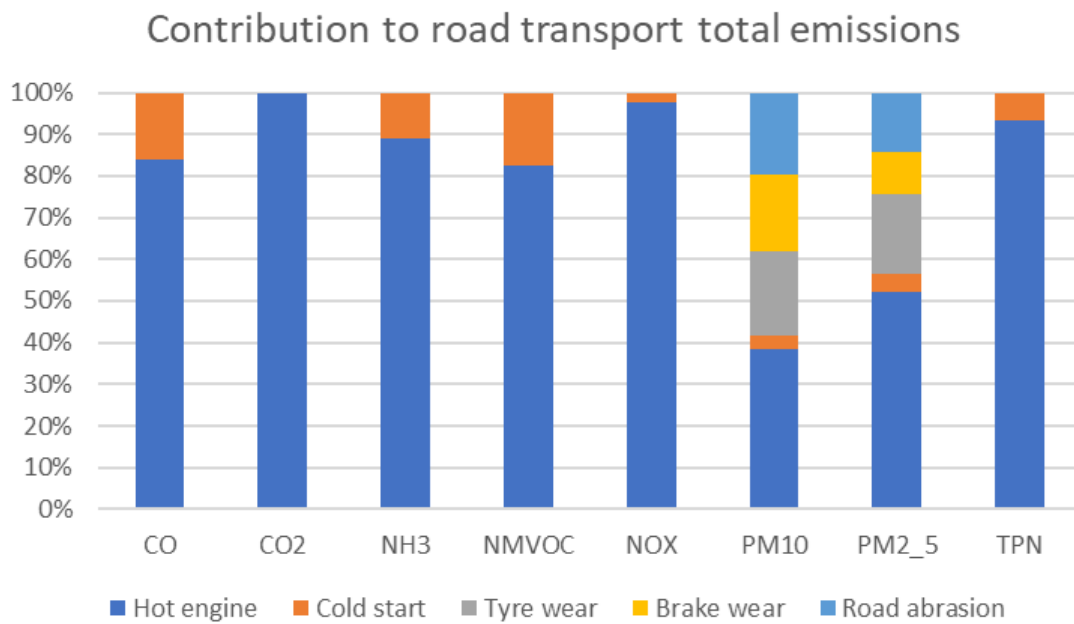


**Figure 4.5.** Contribution of different sources in road transport to total emissions for relevant pollutants. Exhaust emissions are split between hot engines and cold start contribution. TPN, total particle number, equivalent to UFP number concentrations (ST15).

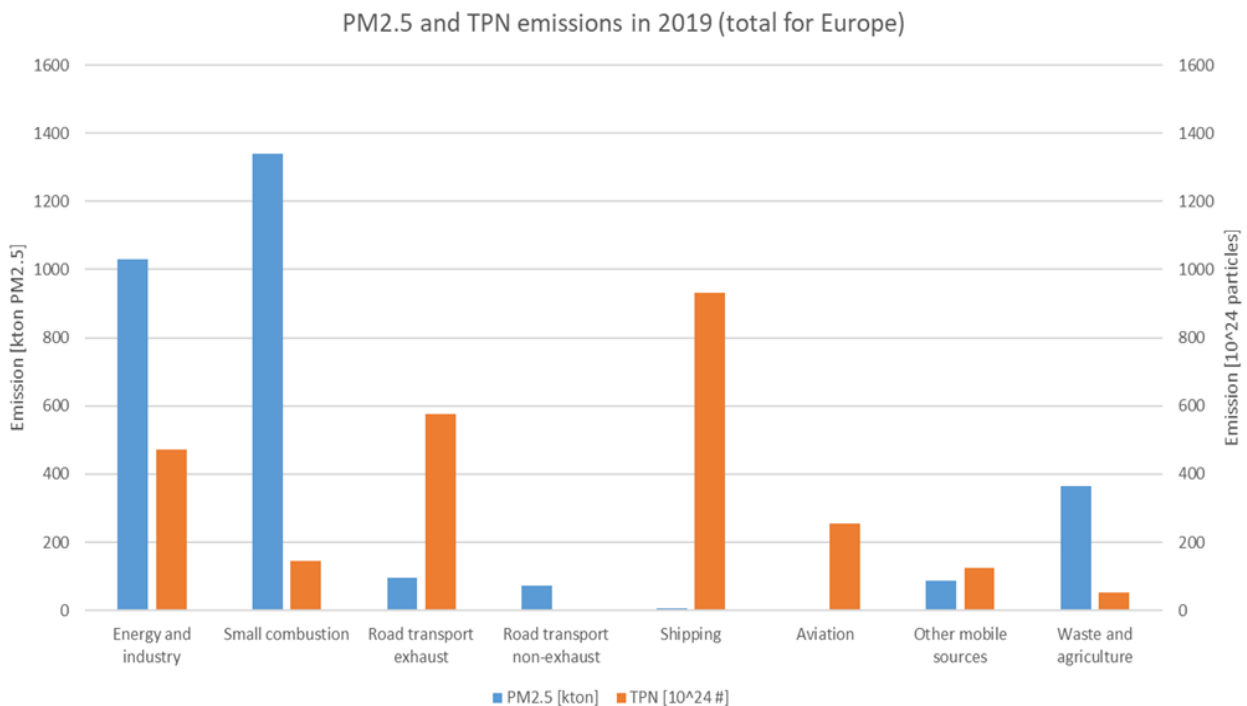


**Figure 4.6.** Comparison between PM<sub>2.5</sub> (in ktons) and total particle number (TPN, equivalent to UFP) emissions (in  $10^{24}$  #) (ST15).

#### 4.1.2. Modelling of UFP and PNSD

**ST16** is a guidance document for the multiscale modelling of UFP-PNSD using deterministic tools. Here an example is presented for the Athens region using PMCAMx-UF. This is a three-dimensional chemical transport model that simulates both the PNSD and the mass/composition distribution of the multicomponent atmospheric aerosol (Jung et al., 2010). The simulation of the aerosol microphysics is handled by the updated version of the Dynamic Model for Aerosol Nucleation (DMANx), which includes the processes of condensation, evaporation, nucleation, and coagulation assuming an internally mixed aerosol (Patoulias et al., 2015). DMANx includes the Two-Moment Aerosol Sectional (TOMAS) algorithm, which tracks both mass and number concentrations simultaneously and can use the desired nucleation theory to simulate particles starting from nuclei sizes.

Figure 4.7 displays the UFP source contributions (in %) over Athens for the summer. The major contributor to UFP is nucleation for the whole modelling domain while diesel also has an important impact in the city centre, and shipping has a great effect on the number concentration on the coast of Athens.

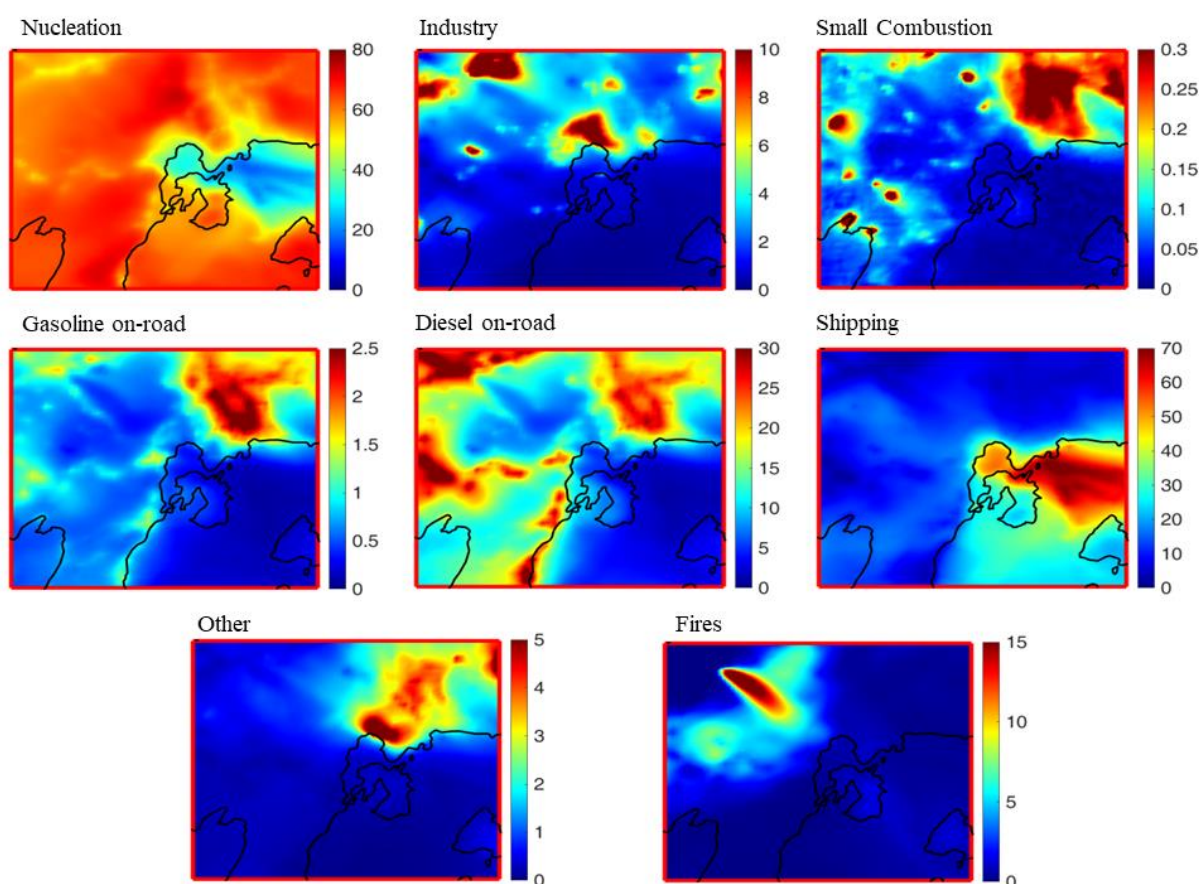


**Figure 4.7.** Predicted source contributions of UFP to the total size range of 10–800 nm ( $N_{10-800}$ ) over Athens for the summer of 2019 using PMCAMx-UF. Domestic biomass burning emissions are not included.

#### 4.1.3. Specific challenges in UFP and PNSD

Long-term measurements of UFP-PNSD are difficult due to complex instrumentation and >90% data coverage is a challenge. Recently, [Hopke et al. \(2024\)](#) and [Vörösmarty et al. \(2024\)](#) carried out studies that cover 15 and 11 years of data, respectively, with a high data coverage. Also, data coverage reported by [Trechera et al. \(2023\)](#) for sites from Budapest, Helsinki, Ispra, Leipzig, Mulheim, Paris, Rochester, reached >90% data coverage but the other 22 sites included in the study did not. A specific attention should be placed on maintenance and follow-up of the UFP and PNSD instruments to reach the required data coverage.

Reliable measurement of UFP and PNSD requires specific sampling as the UFP are rapidly lost in long sampling lines. UFP and PNSD measurements require drying of the sampled particles in order to produce harmonized and comparable data.

There are also challenges in having enough trained and skilled personnel, and for covering the associated costs of personnel and instrumentation, as well as for having an appropriate external calibration and traceability.

Emission inventories and modelling still need improvements to accurately reproduce experimental data on UFP-PNSD, but tools are already available and implemented.

#### 4.2. Added value of measuring eBC concentration in Europe

For elementary Black Carbon (eBC) there is not a reference method and needs harmonisation of measurement protocols and data treatment. In the framework of RI-URBANS, [Savadkoobi et al. \(2023\)](#) evaluated the long-term phenomenology of eBC by compiling datasets on eBC mass concentrations from 50 European monitoring sites, covering various periods between 2006 and 2022. These 50 measurement sites included 23 urban background (UB), 18 traffic (TR), 7 suburban background (SUB), and 2 regional background (RB) sites across 29 cities in 11 European countries (Figure 4.8).

The harmonized dataset indicated a significant decreasing trend in eBC mass concentrations between the classification of environments, generally ranked as TR > UB > SUB > RB. However, there were exceptions, such as high eBC values observed at a rural site in the Po Valley (Northern Italy), known for its PM pollution. Average eBC mass concentrations varied from 3.4  $\mu\text{g m}^{-3}$  at a traffic site in Milan, Italy, to 0.17  $\mu\text{g m}^{-3}$  at a regional background site in Hyytiälä, Finland, based on data from 2017–2019. A notable north–south gradient in eBC mass concentrations, in line with other pollutants like NO<sub>2</sub> or PM<sub>2.5</sub>, reflected regional differences in emissions. Seasonal variability in eBC mass concentrations was evident, with the highest levels observed during winter at the above Milan traffic site (5.2 ± 2.8  $\mu\text{g m}^{-3}$ ) and the lowest in summer at the Finnish regional background site (0.1 ± 0.1  $\mu\text{g m}^{-3}$ ).

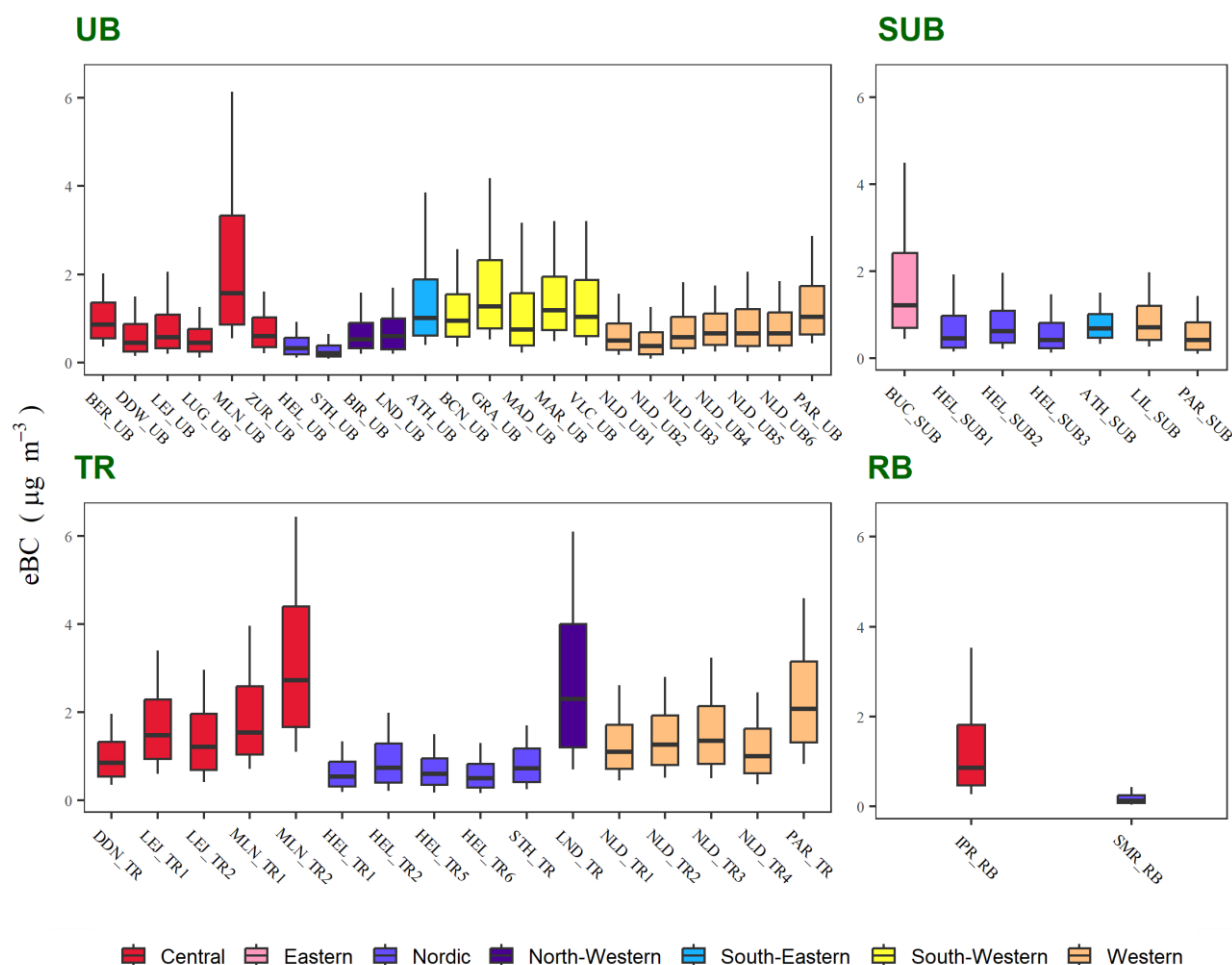


**Figure 4.8.** Variability of hourly averaged eBC mass concentrations at 50 sites between 2017 and 2019 categorized by the type of site and region. Modified from [Savadkoohi et al. \(2023\)](#).

RI-URBANS [ST11](#) provides a methodology for SA allowing to differentiate the BC data to two BC sources, solid fuel emissions and liquid fuel emissions based on the methodology presented in [Sandradewi et al. \(2008\)](#) and ([Zotter et al. 2017](#)). [Savadkoohi et al. \(2024\)](#) gives recommendations for reporting eBC mass concentrations based on long-term pan-European in-situ observations. Figure 4.9 shows the results of the eBC SA in urban Europe provided by [Savadkoohi et al. \(2023\)](#). It shows the regional variations in the relative contributions of eBC from liquid fuels ( $eBC_{lf}$ , mostly road traffic) and eBC from solid fuels ( $eBC_{sf}$ , mostly biomass burning), with an increasing trend in the  $eBC_{lf}$  from Northern to Central, Western, and South-Western Europe.

Long-term observations and SA of BC can allow analysis of trends in emission sources and atmospheric concentrations. For example, Figure 4.10 shows a decreasing trend in  $eBC_{(if)}$  in Barcelona, which is likely a consequence of implementation of diesel particle filters by EURO5/V and 6/VI. On the contrary,  $eBC_{(sf)}$  concentrations follow an increase at the sites influenced by domestic burning. The long-term observations of eBC in the urban areas will allow quantification of impacts of vehicle fleet electrification as the eBC emissions will likely continue to decrease as the combustion engines will become sparser.

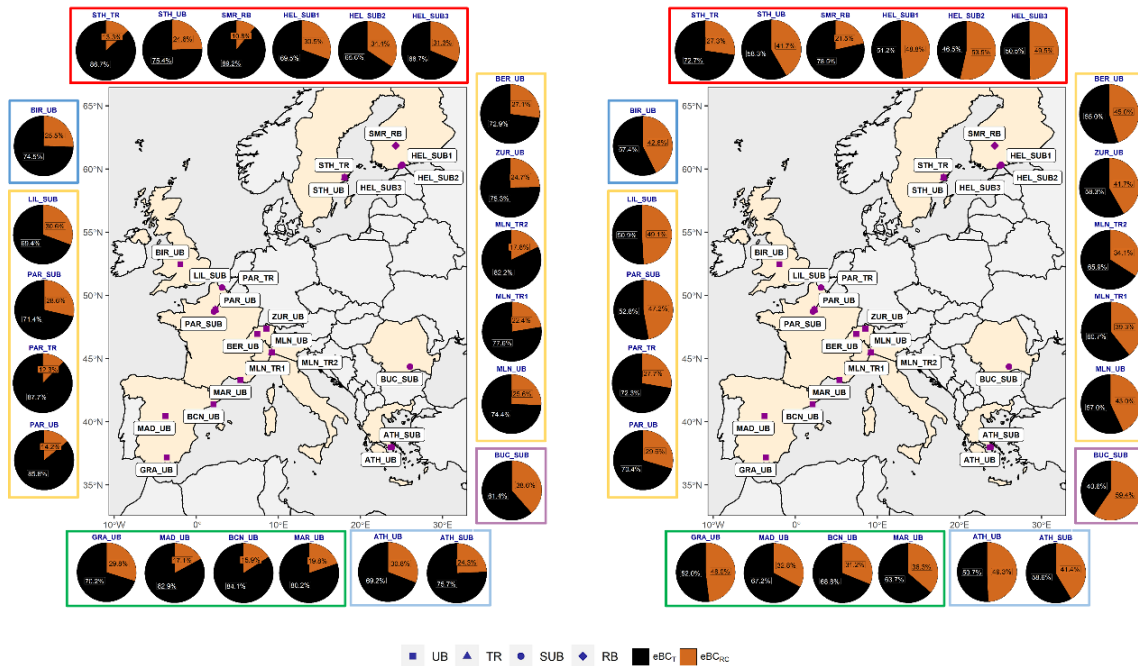


Figure 4.9. The results of the analysis of eBC mass concentrations for 23 European sites used over 2017–2019. Modified from Savadkoohi et al. (2023).

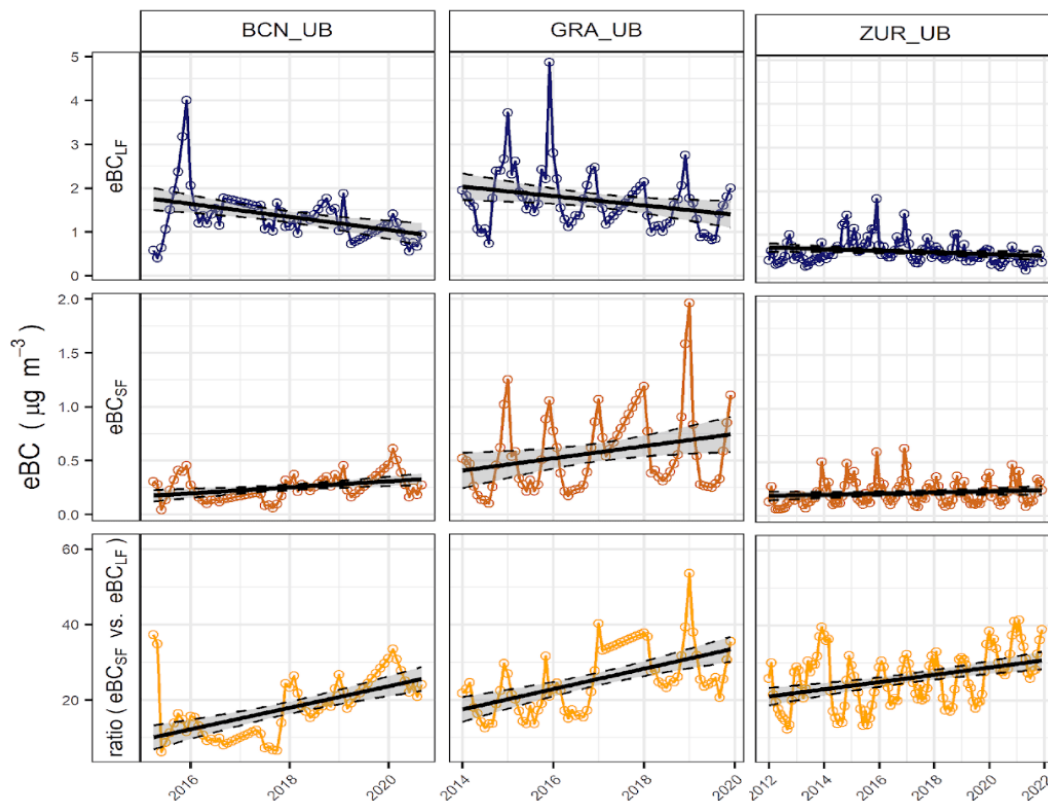


Figure 4.10. The results of the 2012–2022 trend analysis of eBC<sub>f</sub> and eBC<sub>sf</sub> mass concentrations, and the ratio among these, for urban background sites of Barcelona, Granada and Zurich (BCN, GRA, ZUR). Figure from Savadkoohi et al. (2023).

Spatial mapping of BC in the urban areas can be explored with the help of citizen science as some of the BC measurements outside the supersites can be done with small BC sensors. In RI-URBANS, the citizen science approach is summarized in **ST13** (mapping UFP and citizen science). This approach can raise awareness of the urban citizens to air pollution issues.

The observations on BC concentrations together with other air pollutants will enable quantification of health impacts in an unprecedented manner. BC particles are linked to toxicity and the exposure to traffic related BC will likely decrease in the coming decades.

### 4.3. PM speciation and source apportionment in urban Europe using off-line PM measurements

#### 4.3.1. Off-line PM speciation

The major constituents of PM are classically differentiated as follows:

- **Mineral matter** consists mostly of oxides of elements, such as Si, Al, Fe, Ca, Na, Mg, K, Ti, P, and Mn, arising from wind production of suspended soil particles (desert dust, pavement erosion), construction and demolition work, in addition to some industrial emissions (such as the ceramic and cement industry). The maximum of mineral matter emissions is usually in the coarse mode.
- **Sea salt** is mostly composed of  $\text{Cl}^-$  and  $\text{Na}^+$  together with a fraction of  $\text{SO}_4^{2-}$  and  $\text{Mg}^{2+}$ . These have a dominant mode in the coarse fraction.
- **Organic matter (OM)** is a very complex mixture of organic compounds arising from primary combustion sources e.g. hydrocarbons from vehicle exhaust emissions, levoglucosan and polyaromatic hydrocarbons from biomass burning, and many other compounds such as nicotine from smoking and azelaic acid from cooking. In addition, organic matter includes secondary compounds such as carboxylic acids formed from oxidation of gaseous precursors in the atmosphere and polymers of those. OM primarily occurs in the fine fraction.
- **Elemental carbon (EC)** is graphitic or amorphous carbon produced by incomplete combustion of fuels, from vehicles, biomass and coal burning. EC dominant mode is in the fine fraction.
- **Inorganic ions  $\text{NO}_3^-$ ,  $\text{SO}_4^{2-}$ , and  $\text{NH}_4^+$**  constitute the secondary inorganic aerosol (**SIA**) from the atmospheric oxidation of gaseous  $\text{NO}_x$  and  $\text{SO}_2$ , respectively, followed by a reaction with gaseous  $\text{NH}_3$ . These occur as  $\text{NH}_4\text{NO}_3$ ,  $\text{NH}_4\text{HSO}_4$  and/or  $(\text{NH}_4)_2\text{SO}_4$  in the fine fractions of PM. The two first precursors arise from emission of combustion processes, while  $\text{NH}_3$  is primarily emitted from agriculture and farming ([EEA, 2022](#)). Part of the  $\text{Cl}^-$  can contribute to SIA in the form of  $\text{NH}_4\text{Cl}$  in regions where anthropogenic HCl emissions are relevant. These have a dominant mode in the fine fraction. SIA can occur in the coarse mode where  $\text{NaNO}_3$  can form from nitric acid and sea salt.
- **Trace elements** consist of a wide variety of elements (such as As, Cd, Ni, Pb, V, Zn) with different origin, toxicity and size distribution, present in the low concentration (in the  $\text{ng m}^{-3}$  range). The sources of trace elements include e.g. combustion, non-exhaust emissions (tyre dust, brake dust), exhaust emissions, and industrial emissions. These have a dominant role typically in the fine fraction, but those from traffic have a high load in the coarse mode. These and some organic compounds, such as PAHs are key components in PM speciation because some are carcinogenic and others have relevant toxic effects; but also, because these are key tracers for advanced SA studies using receptor modelling.
- **Undetermined fraction** is the PM mass determined by gravimetry that is not accounted for by the sum of the concentrations of all the above PM components, because there are light atoms (typically H, N, O) whose contributions are not properly determined. For instance, crystallisation water accounts for 21% of gypsum

(CaSO<sub>4</sub>·2H<sub>2</sub>O) molecular mass. PM bound water can still contribute significantly to the gravimetric mass if hygroscopic constituents are present. Furthermore, there might be heteroatoms that are not properly quantified in e.g. organic matter.

RI-URBANS compiled datasets of trace elements from 55 sites provided by AQMNs, research projects, and research supersites ([Liu et al., 2024a, 2025a](#)). The datasets span a decade, covering the years 2013 to 2022, with a series of data for each site covering a minimum of one year. The data come essentially from 7 countries: France (24 sites), Italy (9), Spain (8), Switzerland (5), UK (5), Portugal (3), and Greece (1). Thus, the first result from the analysis of this compilation is the scarcity of long-term detailed PM speciation datasets in urban Europe. Details of the datasets, measurement protocols and species analysed are given in [ST3](#).

### Major PM components

In the UB sites, OC had an average concentration (of the averages of the sites) of 6.0±5.4 µg m<sup>-3</sup>, EC around 1.3±1.3 µg m<sup>-3</sup>, NO<sub>3</sub><sup>-</sup> 2.2±3.0 µg m<sup>-3</sup>, SO<sub>4</sub><sup>2-</sup> 1.8±1.4 µg m<sup>-3</sup> and NH<sub>4</sub><sup>+</sup> around 0.82±1.1 µg m<sup>-3</sup>. Median concentrations of Ca<sup>2+</sup>, Fe, Na<sup>+</sup>, Cl<sup>-</sup>, Al, K<sup>+</sup>, and Mg<sup>2+</sup> reached around 0.40±0.44, 0.40±0.40, 0.33±0.49, 0.30±0.70, 0.25±0.38, 0.18±0.24, and 0.04±0.05 µg m<sup>-3</sup>, respectively.

Overall, the concentration of major PM<sub>10</sub> constituents varied across different environment types (Table 5.1), reflecting the influence of specific human activities and natural processes. Specifically, the concentrations of OC and EC were observed to be higher in UB, TR, UI (urban industrial), and SUB environments compared to RB areas, resulting from higher emissions from combustion sources (e.g. traffic, industries, and residential heating) at the former. At RB sites, the OC/EC ratio is significantly higher than at other site types, reflecting the larger contribution to OC from both anthropogenic and biogenic SOA. Thus, a high proportion of OC has a regional origin, while EC is more local (traffic and biomass burning).

For metal ions and elements, the concentrations of Na<sup>+</sup>, Mg<sup>2+</sup>, Al, and Fe were higher at UI and TR environments due to industrial and vehicular emissions. Intermediate concentrations were found in UB and SUB due to the influence of traffic and construction activities. In contrast, RB areas had lower metal ion and element concentrations, resulting from less industrial activity and lower traffic density. K<sup>+</sup> and Ca<sup>2+</sup> concentrations were higher in SUB, UB, and UI due to more biomass burning and construction activities compared to rural areas. Chloride (Cl<sup>-</sup>) concentrations were higher in UI due to industrial processes, with intermediate levels in TR and SUB, and the lowest in RB. In terms of secondary inorganic compounds, SO<sub>4</sub><sup>2-</sup> concentrations did not show significant differences across environments, reflecting that SO<sub>4</sub><sup>2-</sup> is formed from the oxidation of SO<sub>2</sub>, and mainly produced by cloud processing, which is actually a large-scale process. NO<sub>3</sub><sup>-</sup> and NH<sub>4</sub><sup>+</sup> concentrations were higher in TR and RB most probably due to the proximity of the vehicle emissions and the high NH<sub>3</sub> concentrations found in some RB sites due to agriculture and farming emissions ([Liu et al., 2024a](#)), respectively, with intermediate levels in UB and UI, and lowest in SUB.

Table 4.1 shows the average concentration range of major PM components, considering the average for each site for the IND, TR, UB, SUB, and RB sites, for PM<sub>10</sub> and PM<sub>2.5</sub>. The ranges of the two PM sizes are not directly comparable because not many sites are reporting PM<sub>10</sub> and PM<sub>2.5</sub> data. However, the table might be used as a reference of the usual concentrations found in the different environments.

**Table 4.1:** Average concentration range of major PM components, considering the average for each site for industrial (IND), traffic (TR), urban background (UB), suburban background (SUB) and regional background (RB) sites, in  $\mu\text{g m}^{-3}$ , for PM10 and PM2.5. ND, not determined. Data from [Liu et al. \(2025a\)](#).

	PM <sub>10</sub>					PM <sub>2.5</sub>				
	IND	TR	UB	SUB	RB	IND	TR	UB	SUB	RB
OC	2.2-6.0	2.9-18*	2.1-19*	2.4-33*	1.8-2.3		1.9-4.3	1.0-4.9	2.7-5.4	
EC	0.7-2.1	0.3-4.6*	0.2-4.5*	0.4-3.9	0.2-0.2		0.6-1.4	0.2-1.2	0.3-1.1	
SO <sub>4</sub> <sup>2-</sup>	1.7-3.8	1.2-3.1	0.7-2.8	0.5-4.0	2.0-2.2		0.5-1.7	0.5-2.0	1.5-3.1	
NO <sub>3</sub> <sup>-</sup>	1.1-6.5	1.2-6.4	0.7-7.9*	0.7-5.4	3.0-3.2		0.1-5.1	0.1-6.9*	0.2-0.8	
NH <sub>4</sub> <sup>+</sup>	0.1-2.3	0.3-2.4	0.2-3.3*	0.1-1.7	1.2-1.3		0.4-1.9	0.5-2.4*	0.6-0.8	
Cl <sup>-</sup>	0.2-0.4	0.1-3.5	0.2-1.2	0.3-0.8	ND		<0.1-0.1	<0.1-0.1	<0.1-0.1	
Na	0.4-1.3	0.1-2.0	0.1-0.9	0.2-0.8	ND		<0.1-0.1	<0.1-0.1	0.1-0.1	
Mg	0.2-0.4	0.1-0.4	<0.1-0.9	0.1-0.4	ND		0.1-0.02	<0.1-0.6	<0.1-0.2	
Ca	1.7-2.7	0.3-1.2	0.2-1.6	0.2-0.8	ND		<0.1-0.2	0.1-0.2	0.1-0.2	
Si	ND	0.3-1.3	0.2-1.3	0.2-1.0	ND		<0.1-0.1	0.1-0.7	0.1-0.3	
Al	0.1-1.3	0.1-0.8	<0.1-1.1	<0.1-0.6	0.1-0.1		<0.1-0.1	<0.1-0.2	<0.1-0.1	
Fe	0.3-3.9	0.3-1.4	0.1-1.2	<0.1-1.1	0.1-0.2		0.1-0.5	<0.05-0.2	0.1-0.1	
K	0.2-1.4	0.2-0.4	0.2-1.3	0.2-1.5	ND		0.1-0.5	<0.05-0.6	0.1-0.2	
Levogluconan	0.1-0.3	0.2-0.8	0.1-3.2*	0.2-0.9	0.1-0.1		<0.1-0.3	<0.1-1.1	<0.1-0.3	

## Trace elements

Twenty trace elements in PM10 were selected for this overview, including As, Ba, Br, Cd, Co, Cr, Cu, Hg, Mn, Mo, Ni, Pb, Rb, Se, Sr, Ti, V, Y, Zn, and Zr. Among these, Cd, As, Cr, and Ni are classified as carcinogenic elements ([WHO, 2007](#)). It is worth mentioning that Sn and Sb were not included because these elements were not determined or detected in a number of sites where wet chemistry methods were not applied, but these are relevant for SA analyses.

AQ limit/target values for trace elements in European AQ Directives are set up only for As (6 ng m<sup>-3</sup>), Pb (500 ng m<sup>-3</sup>), Cd (5 ng m<sup>-3</sup>), and Ni (20 ng m<sup>-3</sup>) listed in 2008/50/EC and 2004/107/CE. The average concentrations of As, Pb, Cd, and Ni all complied with EU standards. The highest concentrations were recorded for Zn, Cu and Ti (40±48, 23±34 and 20±29 ng m<sup>-3</sup>, respectively), followed by Mn and Ba (12±25 and 11±15 ng m<sup>-3</sup>, respectively), all of them being conventionally attributed to brake-wear, tyre-wear and road dust resuspension in urban environments (Amato et al., 2016). Inhalation of these trace elements poses significant health risks. For instance, As, Cd, and Ni are known carcinogens, with exposure linked to lung and bladder cancers ([WHO, 2007](#)). Zn, Cu, and Mn, while essential in small amounts, can cause toxicity at higher concentrations, leading to respiratory and cardiovascular problems ([Wu et al., 2019](#)). Overall, the presence of these toxic metals in PM highlights the need for stricter regulatory measures and continuous monitoring to mitigate adverse health effects on urban populations. Table 4.2 shows the average concentration range of trace elements, considering the average for each site for the IND, TR, UB, SUB, and RB sites, for PM10 and PM2.5.

**Table 4.2:** Average concentration range of trace elements, considering the average for each site, in industrial (IND), traffic (TR), urban background (UB), suburban background (SUB) and regional background (RB) sites, in  $\text{ng m}^{-3}$ , for PM<sub>10</sub> and PM<sub>2.5</sub>. ND, not determined. Data from [Liu et al. \(2024b\)](#).

	PM <sub>10</sub>					PM <sub>2.5</sub>				
	IND	TR	UB	SUB	RB	IND	TR	UB	SUB	RB
As	<0.1-10	<0.1-9.2	<0.1-7.9	<0.1-28	<0.1-4.1		0.2-0.7	<0.1-1.6	<0.1-0.4	
Ba	<0.1-61	<0.1-133	<0.1-416	<0.1-344	0.1-20		<0.1-6.7	<0.1-24.7	4.0-7.9	
Br	<0.1-2.3	<0.1-734	<0.1-160	<0.1-23	<0.1-3.0		ND	ND	ND	
Cd	<0.1-6.6	<0.1-5.2	<0.1-9.3	<0.1-7.0	<0.1-0.7		<0.1-0.2	<0.1-0.1	3.2-3.7	
Co	<0.1-2.7	<0.1-2.2	<0.1-47	<0.1-110	<0.1-0.2		<0.1-0.1	<0.1-0.1	<0.1-0.1	
Cr	<0.1-32	<0.1-51	<0.1-200	<0.1-122	<0.1-34		0.5-2.3	<0.1-2.9	0.8-1.3	
Cu	<0.1-349	<0.1-215	<0.1-1087	<0.1-117	<0.1-1.5		7.9-15	0.7-16.2	2.4-5.1	
Hg	<0.1-55	<0.1-216	<0.1-50	0.5-56	0.1-35.2		ND	ND	ND	
Mn	<0.1-118	<0.1-149	<0.1-185	<0.1-91	<0.1-28		2.1-7.8	0.1-3.8	2.0-3.3	
Mo	<0.1-46	<0.1-177	<0.1-57	<0.1-5.0	<0.1-0.1		<0.1-3.2	<0.1-16	<0.1-22	
Ni	<0.1-95	<0.1-261	<0.1-64	<0.1-318	<0.1-0.1		<0.1-0.9	<0.1-2.5	1.6-4.9	
Pb	<0.1-967	<0.1-312	<0.1-306	<0.1-149	<0.1-3.6		0.8-5.2	0.5-4.9	2.6-4.4	
Rb	0.1-15	<0.1-45	<0.1-35	<0.1-18	<0.1-8.1		0.2-1.3	0.1-1.3	0.5-0.9	
Se	<0.1-62	<0.1-32	<0.1-211	<0.1-57	0.1-119		<0.1-0.1	<0.1-0.1	0.4-0.5	
Sr	<0.1-92	<0.1-130	<0.1-147	<0.1-100	<0.1-1.8		<0.1-5.2	<0.1-16	0.7-1.5	
Ti	<0.1-516	<0.1-620	<0.1-345	0.1-521	<0.1-1.6		0.7-6.1	<0.1-0.1	3.3-10	
V	0.1-118	<0.1-34	<0.1-64	<0.1-23	0.2-4.7		0.1-0.3	<0.1-0.5	1.5-2.9	
Y	<0.1-2.8	<0.1-11	<0.1-7.6	<0.1-3.0	ND		<0.1-0.3	<0.1-0.3	ND	
Zn	<0.1-1034	0.1-575	<0.1-1983	<0.1-356	1.8-56		7.0-26	3.5-30	9.2-11	
Zr	<0.1-23	<0.1-23	<0.1-18	<0.1-10	ND		<0.1-5.2	<0.1-8.1	<0.1-11	

#### 4.3.1.1. Source apportionment based on off-line PM speciation

Source receptor modelling using Positive Matrix Factorisation (PMF, [Paatero and Tapper, 1994](#); [Paatero and Hopke, 2009](#)) was applied to the off-line PM speciation datasets compiled. [Liu et al. \(2025a\)](#) and [ST10](#) report details of the protocols recommended and applied to this end. As shown in Figure 4.11, solutions with 5–9 PM<sub>10</sub> factors (source contributors) provided the most suitable and reliable outcomes across the 24 monitoring sites, which were identified. In summary, sources of ambient PM<sub>10</sub> have been grouped into 7 categories:

- Road traffic (including exhaust and non-exhaust vehicle emissions).
- Biomass burning.
- A crustal source.
- SIA+SOA.
- Industrial sources.
- Sea-salt source (in most cases loaded with aged anthropogenic PM).
- A mixed fuel-oil combustion (with or without shipping).
- Other specific sources.

Their source contributions to PM<sub>10</sub> for each city widely vary according to local and regional emission patterns and climate characteristics. Details of the datasets, source profiles and locations are given in [Liu et al. \(2025a\)](#).

These results suggest that EU-wide offline PM speciation datasets can support advanced policy assessments at EU, regional, and local levels. Additionally, policies aimed at reducing PM may need to be tailored to the specific climates and cities across Europe. In Central Europe, nitrate (deep blue in Figure 4.11) makes a significant contribution to PM, whereas its contribution is much lower in Southern Europe. Road traffic (black in the figure) is a notable source of PM<sub>10</sub> across all cities, though its contribution varies widely. Biomass burning is a major source in most locations, and in many cases, it is the largest contributor.

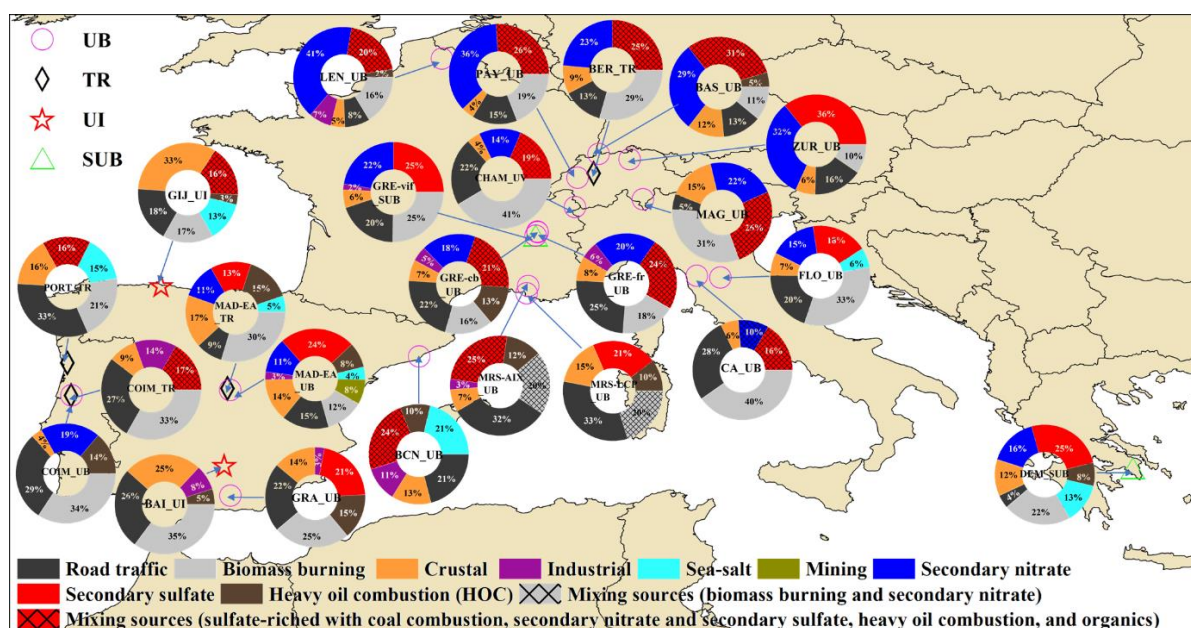


**Figure 4.11.** Quantitative source apportionment (with PMF) of mean PM<sub>10</sub> concentrations for 24 locations across 6 countries in Europe. Figure from [Liu et al. \(2025a\)](#).

### 4.3.2. Non-refractory PM<sub>1</sub> speciation and source apportionment in urban Europe using on-line PM measurements

#### 4.3.2.1. On-line PM speciation

RI-URBANS also compiled available datasets of urban long-term measurements of the non-refractory (NR) PM<sub>1</sub> measured with Aerosol Chemical Speciation Monitors (ACSM). These datasets were obtained in the period covering from 2011 to 2023, with different duration, and were provided to RI-URBANS by AQMNs, RIs (such as ACTRIS) and single research institutes. These included 26 UB sites, and additionally 5 SUB, 3 TR and 1 RB sites.

Regarding NR-PM<sub>1</sub> composition, the main component was organic aerosol (OA) at all sites. The average, standard deviation, and ranges (average  $\pm$  standard deviation, min–max %) of each species (for a set of sites excluding Birmingham (PM<sub>2.5</sub> instead of PM<sub>1</sub>) and without stations, were:

- OA: 55 $\pm$ 10%, 40–67%
- SO<sub>4</sub><sup>2-</sup>: 18 $\pm$ 8%, 9–48%
- NO<sub>3</sub><sup>-</sup>: 16 $\pm$ 5%, 6–26%
- NH<sub>4</sub><sup>+</sup>: 10 $\pm$ 3%, 5–19%

- Cl<sup>-</sup>: 1±1%, <0.1–6%

The 35 sites were classified into four groups according to the chemical compositions shown in Figure 4.12:

- SO<sub>4</sub><sup>2-</sup> << NO<sub>3</sub><sup>-</sup>: Typically, continental or high-latitude sites, where winter stagnation episodes are frequent and/or severe, or with high traffic influence.
- SO<sub>4</sub><sup>2-</sup> >> NO<sub>3</sub><sup>-</sup>: Typically, with sea influence and in lower latitudes, where SO<sub>4</sub><sup>2-</sup> is photochemically produced from dimethyl sulphide and/or shipping emissions.
- SO<sub>4</sub><sup>2-</sup> ≈ NO<sub>3</sub><sup>-</sup>: Typically, intermediate sites, with similar concentrations in summer and winter.
- High Cl<sup>-</sup>: Only three sites (Padova, Milano, Bologna) were identified with high Cl<sup>-</sup>, and this was in the Po Valley region known for elevated PM levels. These three datasets presented very high NR-PM<sub>1</sub> concentrations and high amounts of NO<sub>3</sub><sup>-</sup>, with the exception of Padova which is closer to the coast and more SO<sub>4</sub><sup>2-</sup> dominated. These results can be biased because Padova and Milano data is only for winter, but in any case, the Po Valley is known as a European hotspot for PM accumulation due to the orographic and meteorological conditions, multiple sources of PM and recirculating breeze regimes which cause severe winter pollution episodes (Scotto et al., 2021).

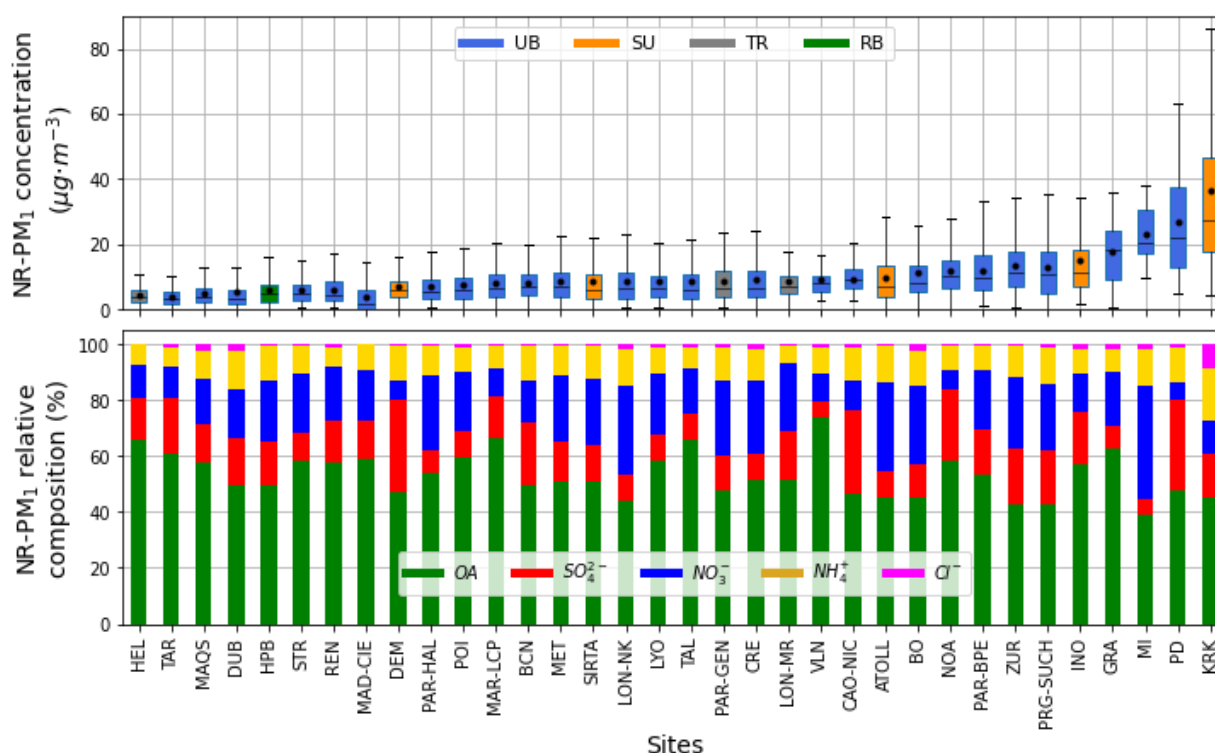


**Figure 4.12.** (a) NR-PM<sub>1</sub> concentrations boxplots. (b) Relative composition of NR-PM<sub>1</sub> compounds. Both graphs are ordered by growing mean concentration of NR-PM<sub>1</sub>. Upper: Concentration boxplots include average (circle), median, quartiles 25 and 75%, and minimum and maximum. Lower: Relative composition of NR-PM<sub>1</sub> compounds. Both graphs are ordered by growing mean concentration of non-refractory-PM<sub>1</sub>.

#### 4.3.2.2. Source apportionment based on on-line PM speciation

PMF-ME2 receptor modelling was applied to 19 datasets of NR-PM1 on-line speciation measurements (see [ST10](#) for detailed methodology used) for OA apportionment. Primary sources of the OA include hydrocarbon like OA (HOA, and also HOA1, HOA2), biomass burning OA (BBOA), cooking-like OA (COA), amine OA (amine-OA), wood, coal, and peat OA, coal combustion OA (Coal OA), shipping + industry OA (ShINDOA), local OA (LOA); primary OA (POA), and cigarette-smoke OA (CSOA). Amongst secondary OA there are less-oxidised oxygenated OA (LO-OOA), more-oxidised oxygenated OA (MO-OOA), and generic oxygenated OA (OOA). Also, there are different mixings of OOA+BB (OOA\_BB, OOA\_BBaq).

The proportion of SOA amongst all the sites was 41–92% of the OA, with a mean and standard deviation of 65% and 13%, respectively. As it can be seen in Figure 4.13 the regional background site, Hohenpeissenberg, was the one with the lowest proportion of primaries, as expected from remote background sites. Contrarily, the urban background sites presented the minimum SOA/OA ratios, even though there is a high variability of sources amongst sites.

For POA there were a few sites whose BBOA was the dominant POA. All the Po Valley sites were POA-BBOA-dominated. Conversely, although traffic was not the main primary source at almost any site (HOA), it was present at every site, even in the remote background ones, implying that traffic was not only a local source but also an OA source of regional influence. In addition, COA was also a relevant source, especially in urban background locations and in one traffic site, but it was not detected at suburban sites. This implied that this source was unstable under transport conditions from the most densely populated areas to city outskirts. Coal combustion was a relevant source only in Dublin and Krakow, although in the latter it was the most prominent primary source. Other primary sources present in this study in minor proportions were amine-OA, wood and peat burning, Shipping + Industry OA, local OA, a generic primary OA source, and cigarette smoke OA.

Regarding SOA, all sites achieved the differentiation of two main SOA factors differentiated upon their degree of oxidation into Less Oxidised-OOA and More Oxidised-OOA, except for the Granada and Padova sites, probably because of the campaigns being short and in winter. In summer, according to various SA studies, the OOA is easy to differentiate, with the formation of LO-OOA due to the enhancement of photochemical reactions and of MO-OOA which denotes a more aged and regional origin ([Via et al., 2021](#)). In Zurich, both OOA and LO-OOA/MO-OOA pairs were present because both SOA factors were differentiated in the warmer periods but not in the colder seasons. The Bologna site also achieved the differentiation of two more OOAs related to BBOA emissions giving the capacity of the aerosol mass spectrometer (AMS) to resolve individual species.

Details of the datasets, source profiles and specific SA results are given in [ST10](#).

The results show clearly that NR-PM1 on-line speciation measurements and SA applied to the resulting dataset is a very useful tool to determine the source contributions to OA, a main (if not the main) PM2.5 component, and assess policies for PM abatement. Even if measurements are done for PM1 for measurement protocols, the OA of PM2.5 and PM1 are mostly equivalent. Furthermore, it can inform AQMNs managers on a NRT mode to show the composition and SA of PM in specific pollution episodes and then support policy decisions for short term actions.

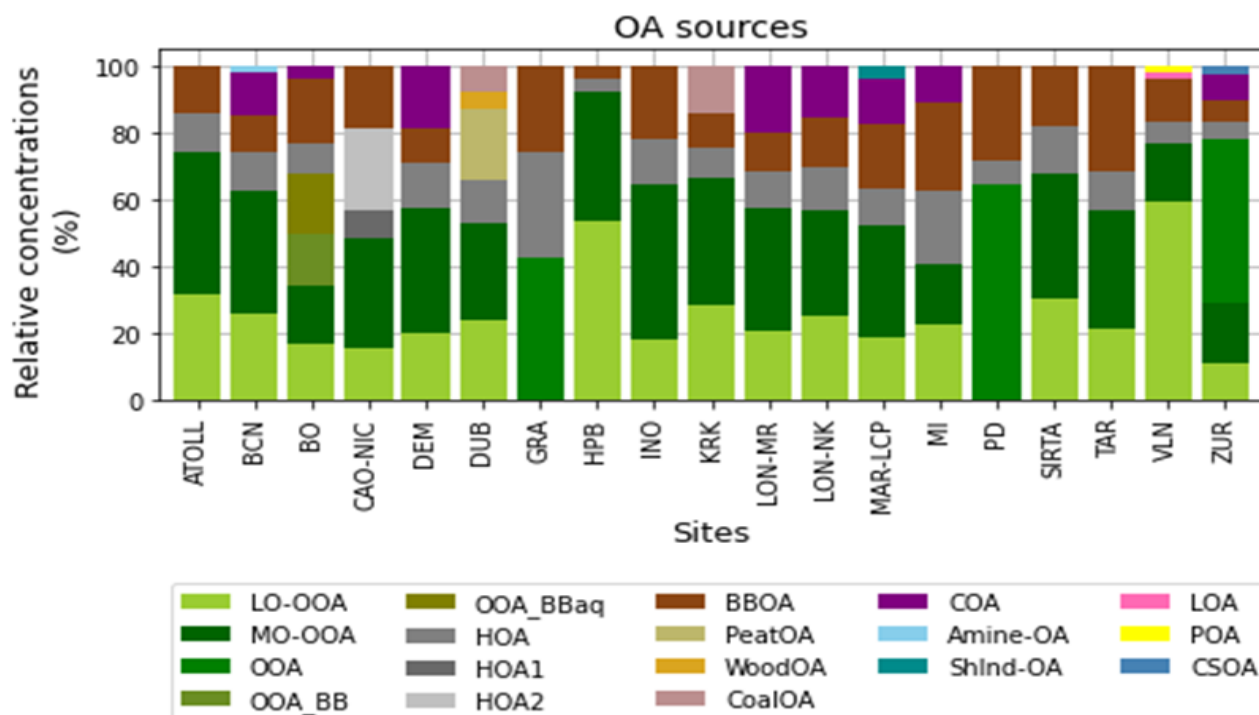


Figure 4.13. Relative mean site OA composition of all sites providing source apportionment results.

#### 4.4. Added value of measuring oxidative potential of PM in urban Europe

Health effects attributable to PM are complex and diverse, and overall, PM<sub>2.5</sub> is now considered to be the largest environmental contributor to adverse health effects globally (WHO, 2021). PM may act through different mechanisms such as oxidative stress and inflammation, genomic alterations, impaired nervous system function, epigenetic alterations, among others. Thus, it is not possible to cover all these effects by monitoring a single AQ parameter.

Oxidative potential of particulate matter (OP of PM) represents the capacity of PM to invoke oxidative reactions or to generate reactive oxygen species (ROS) in a biological media (Uzu et al., 2011, among others). The ROS can be carried on by the PM or be induced/produced from their interactions with the biological system (e.g., fluids, cells, and tissues) and be quantified by different methodologies (Sarnat et al., 2016, among others). Oxidative potential can be calculated for different target molecules, such as 1,4-dithiothreitol (OP<sup>DTT</sup>), ascorbic acid (OP<sup>AA</sup>), glutathione (OP<sup>GSH</sup>), uric acid (OP<sup>UA</sup>), and 2,7-dichlorodihydrofluorescein (OP<sup>DCFH</sup>), among the most used. These are known as depletion OP assays (Janssen et al., 2014). Furthermore, the (OP<sup>ESR</sup>) assay measures OP based on the ability of PM to generate hydroxyl radicals (•OH) in the presence of hydrogen peroxide (H<sub>2</sub>O<sub>2</sub>), and the spin trap 5,5-dimethyl-1-pyrroline-N-oxide (DMPO) (Janssen et al., 2014). The OP<sup>OH</sup> assay measures the formation of the radical hydroxyl (•OH) in surrogate lung fluid containing the major lung antioxidants, while the Electron Paramagnetic Resonance (EPR) assay measures particle-bound free radicals (Shen et al., 2022).

OP is usually a kinetic measurement based on the depletion rate of anti-oxidants or surrogates when in contact with PM. OP can be mass-normalised (OP<sub>m</sub>, expressed in nmolAnti-Ox.min<sup>-1</sup>µg<sup>-1</sup>) representing the inherent capacity of one µg of PM to oxidise the lung and is related to the “harmfulness” of such PM. Alternatively, OP can be volume-normalised (OP<sub>v</sub>, expressed in nmolAnti-Ox.min<sup>-1</sup>.m<sup>-3</sup>) related to the exposure of populations to atmospheric

oxidant compounds. Note that OPv of PM is often abbreviated in OP of PM and OPm also called “intrinsic OP” in scientific literature.

**ST4** reviews the available OP measurements and proposes a simplified RI-URBANS measurement protocol with the OP<sup>DTT</sup> assay ([Dominutti, et al., 2024](#)) and also reports on OP<sup>DTT</sup> and OP<sup>AA</sup> levels in urban Europe. Figure 4.14 shows a summary of OP<sup>DTT</sup> and OP<sup>AA</sup> values reported in urban Europe, with the highest ones being reached in road traffic sites and cities with high biomass burning contributions. All these results point out that both OP<sup>AA</sup> and OP<sup>DTT</sup> are sensitive to organic species and metals carried out by PM but to a different extent. In fact, OP<sup>DTT</sup> – a thiol-based assay, displays a more balanced response to all atmospheric compounds than OP<sup>AA</sup>, being more specific to a few specific species (mainly metallic, or biomass-burning compounds related). The combinations of both OP<sup>DTT</sup> and OP<sup>AA</sup> is evaluated as a good approach to characterise OP of PM. However, despite the development of several acellular assays to evaluate OP of PM, there exists a lack of consensus regarding methodologies and protocols for the OP of PM measurement, as well as the quantification and calibration procedures, hindering inter-study comparisons.

In addition to the OP<sup>DTT</sup> simplified tests, an additional OP<sup>AA</sup> simplified test has been developed and soon will be published in scientific journals.

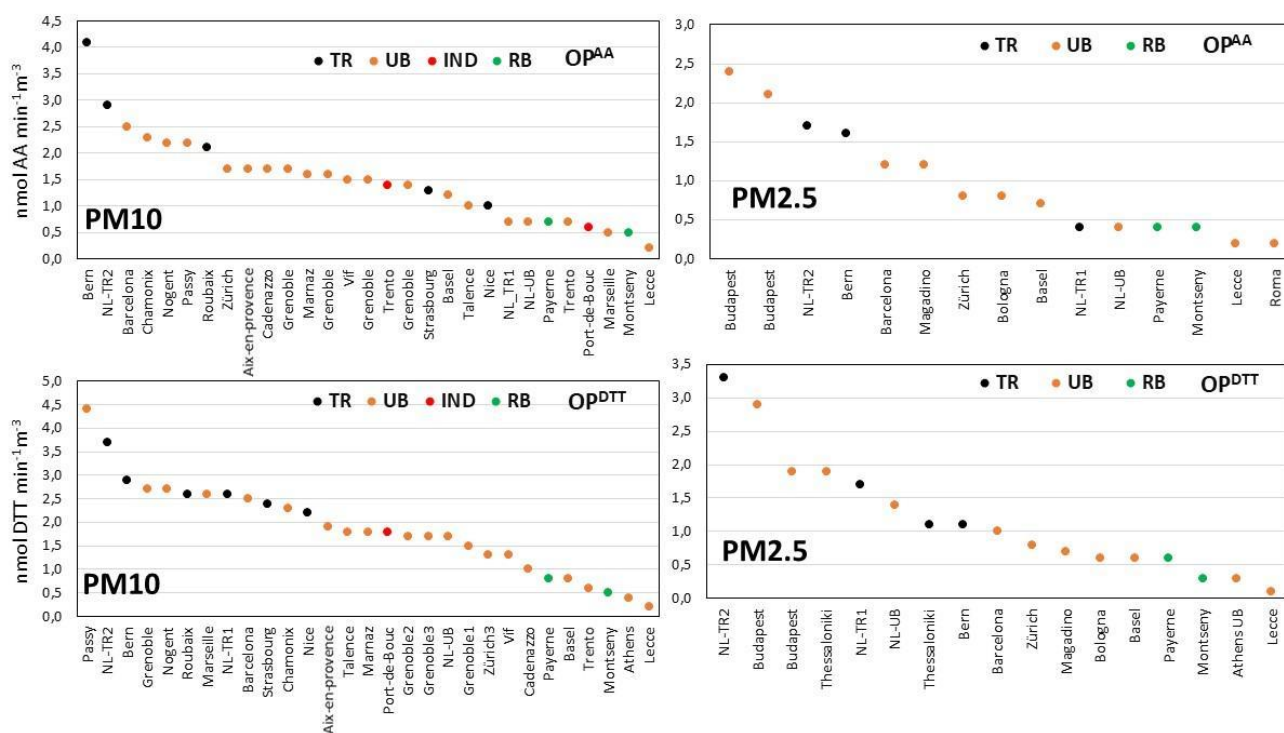


**Figure 4.14.** OP<sup>AA</sup> and OP<sup>DTT</sup> volume of PM mean values (nmol min<sup>-1</sup> m<sup>-3</sup>) in (mostly) urban sites, reported by [Janssen et al. \(2014\)](#), [Argyropoulos et al. \(2016\)](#), [Visentin et al. \(2016\)](#), [Paraskevopoulou et al. \(2019\)](#), [Pietrogrande et al. \(2019\)](#), and references therein, [Weber \(2021\)](#), [Weber et al. \(2021\)](#), [Grange et al. \(2022\)](#), [Dominutti et al. \(2023\)](#), [In 't Veld et al. \(2023a\)](#) and [Vörösmarty et al. \(2023\)](#).

**ST11** reviews the methodology for SA of OP of PM, which is based on PMF SA applied to PM speciation datasets followed by multilinear regression to assign collocated measurements of OP to PMF sources. Figure 6.2 shows results of the SA of OP of PM10 from an urban Alpine city in France ([Dominutti et al., 2023](#)). This included the assessment of well-established assays like AA, DTT, and DCFH, alongside novel assays such as Ferric-Xylenol Orange (FOX) and direct ROS quantification via OH radical. The main findings underscored the significant influence of

seasonality on source contributions and OP activities. In winter, when anthropogenic emissions dominate, all OP assays exhibited strong agreement. Conversely, in warmer months, with reduced anthropogenic influence, biogenic and secondary organic-related aerosols exerted a greater impact. Additionally, we observed varying sensitivities of each OP assay to PM<sub>10</sub> sources, likely reflecting differences in chemical composition and processes ([Dominutti et al., 2023](#), Figure 4.15).

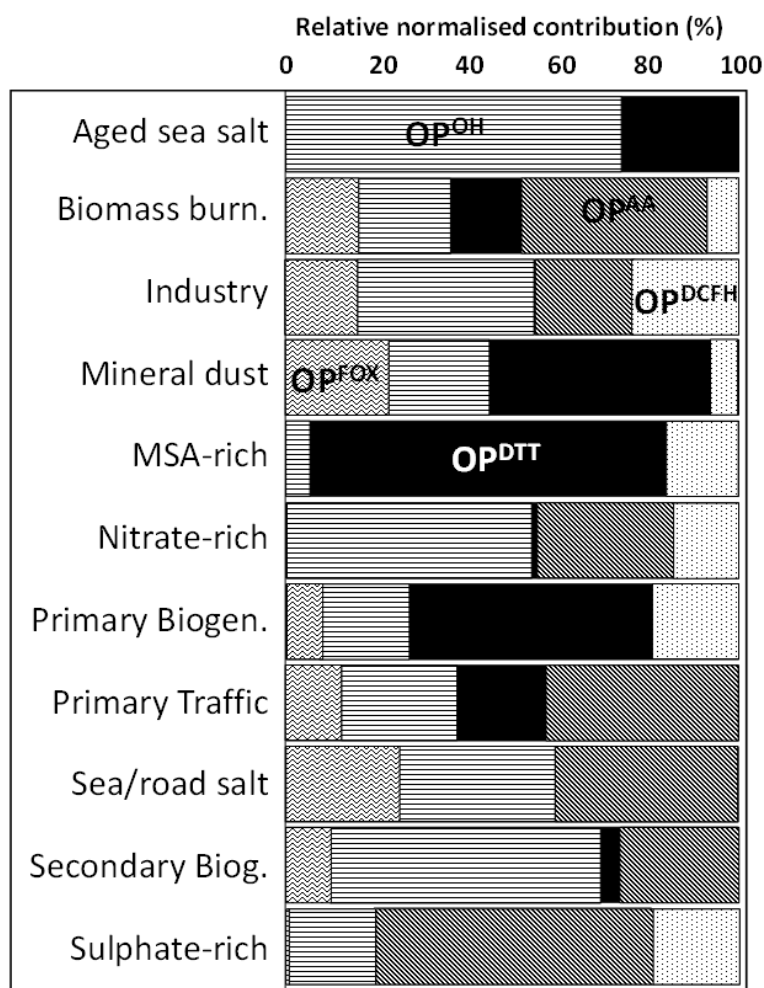


**Figure 6.2:** OP sensitivity contribution of each PM source. Relative normalised contribution of OP assays to the PM<sub>10</sub> sources. Colours represent each OP test evaluated (adopted from [Dominutti et al., 2023](#)).

#### 4.5. The added value of measuring NH<sub>3</sub> in urban Europe

In the urban background areas of European cities, 70% of the PM<sub>2.5</sub> arise from (SIA and SOA ([Amato et al., 2016](#)). Emitted sulphur dioxide (SO<sub>2</sub>) and nitrogen oxides (NO<sub>x</sub>) undergo atmospheric oxidation reactions that generate gaseous sulphuric (H<sub>2</sub>SO<sub>4</sub>) and nitric acid (HNO<sub>3</sub>). Once formed, these react with NH<sub>3</sub> to generate ammonium sulphate (NH<sub>4</sub>HSO<sub>4</sub> and (NH<sub>4</sub>)<sub>2</sub>SO<sub>4</sub>) and ammonium nitrate (NH<sub>4</sub>NO<sub>3</sub>), two major components of PM<sub>2.5</sub> (Figure 4.16). PM<sub>2.5</sub> reduction can become challenging with increasing (or stable) NH<sub>3</sub> concentrations, in situations where NH<sub>3</sub> availability is the limiting factor in SIA formation (i.e. HNO<sub>3</sub> is in excess). Furthermore, NH<sub>3</sub> might interact with VOCs and SOA to produce NH<sub>4</sub><sup>+</sup>-bearing SOA, which contributes to increase the aerosol radiative forcing (brown carbon, BrC; [Bones et al., 2010](#)) and to stabilize SOA in PM ([Paciga et al., 2014](#)). It has been demonstrated the abating NH<sub>3</sub>

emissions is a cost-effective measure for mitigating PM<sub>2.5</sub> (Gu et al., 2021). Furthermore, Lelieveld et al. (2015) attributed premature mortality to NH<sub>3</sub>-derived SIA in Europe, Russia and East Asia, assuming all particles are of equal toxicity. Although in some cases, (NH<sub>4</sub>)<sub>2</sub>SO<sub>4</sub> and NH<sub>4</sub>NO<sub>3</sub> in PM<sub>2.5</sub> are considered as the PM components with the lowest potential for health effects, WHO (2013) stated that there is no evidence to exclude health effects for these components.

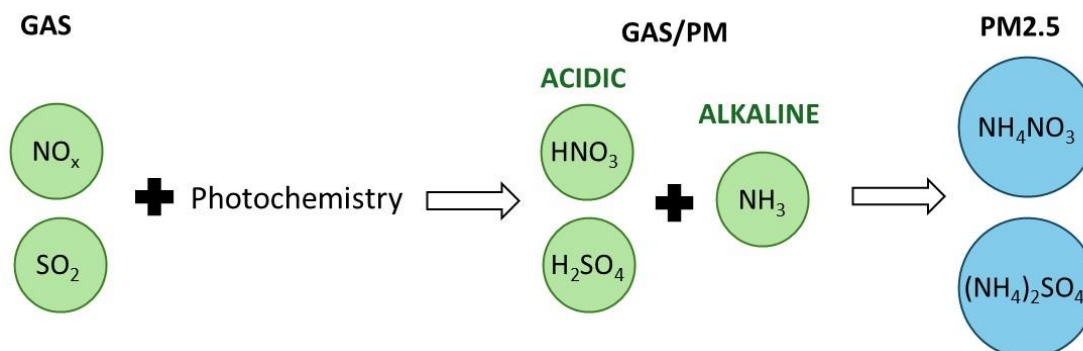


**Figure 4.16.** Atmospheric processes yielding to the formation of secondary inorganic PM<sub>2.5</sub>.

NH<sub>3</sub> might also have important effects on ecosystems by causing foliar injury on vegetation, with a sensitivity that follows native vegetation > forests > agricultural crops (Krupa, 2003). Other impacts on vegetation include growth and productivity, tissue content of nutrients and toxic elements, drought and frost tolerance, responses to insect pests and disease-causing microorganisms (pathogens), development of beneficial root symbiotic or mycorrhizal associations and inter species competition or biodiversity. High levels of nitrogen (N) deposition, due to high NH<sub>3</sub> ((NH<sub>4</sub>)<sub>2</sub>SO<sub>4</sub>, NH<sub>4</sub>HSO<sub>4</sub> and NH<sub>4</sub>NO<sub>3</sub>) contribute to eutrophication of ecosystems by N saturation and the consequent negative effects (Hettelingh et al., 2017).

Unlike the AQ criteria pollutants, NH<sub>3</sub> does not have AQ standards in Europe. However, a number of Member States set thresholds for the protection of vegetation, or recommended targets are proposed (UNECE, 2007; Cape et al., 2009). Thus, UNECE long-term Critical Levels (CLE) have been set at 1 µg m<sup>-3</sup> for lichens and bryophytes and at 3 µg m<sup>-3</sup> for higher plants.

In the EU-27, agriculture and farming are the leading contributors to the NH<sub>3</sub> emission inventory, accounting for 94% of total NH<sub>3</sub> emissions in 2020. Other sources, including industry, road transportation, and solid waste management, each contribute approximately 1% (EEA, 2022). However, in urban and industrial areas, where SO<sub>2</sub> and NO<sub>x</sub> emissions are high, high NH<sub>3</sub> concentrations from local sources might contribute to the increase of PM<sub>2.5</sub>. Relevant urban sources of NH<sub>3</sub> are waste management, traffic and fugitive emissions from sewerage systems (Reche et al., 2012, 2015; Pandolfi et al., 2012).

In urban areas, the contribution of NH<sub>3</sub> derived from traffic sources have a potential for an increase due to the widespread implementation of selective catalytic reduction (SCR) NO<sub>x</sub>-controls in the new EURO 6/VI diesel vehicles (Hopke and Querol, 2022), which uses urea or NH<sub>3</sub> as catalysts to reduce NO<sub>2</sub> tail-pipe emissions. In fact, Reche et al. (2022) reported increases in urban NH<sub>3</sub> concentrations in Barcelona in 2011–2020 probably due to the increase of emissions from traffic and waste management.

In the framework of RI-URBANS, Liu et al. (2024a) compiled 69 datasets of NH<sub>3</sub> concentrations from European regional, suburban and urban background (RB, SUB and UB, respectively), industrial (IND) and traffic sites (TR). These included 36 sites from Spain, 15 from France, 12 from Italy, five from the UK and one from Finland. Most of the data was from non-rural sites (UB, 15; SUB, 12; TR, 12; IND, 5), but although the focus was on urban and farming/agricultural hotspots, 15 RB datasets were also collected to better interpret NH<sub>3</sub> spatial and temporal

variability. Remote sensing data (Van Damme et al., 2018) was used to identify the spatial extension of farming/agricultural NH<sub>3</sub> hotspots (FAHs). Furthermore, arbitrarily, RB sites reaching average concentration >1.5 µg/m<sup>3</sup> were also classified as FAHs, and these were named Regional Background sites Close to Hotspot (RBCH). A wide range of instrumentation was used to measure NH<sub>3</sub> concentrations, including active denuders, passive samplers, online chemiluminescence gas chromatography-mass spectrometry, optical CRDS (cavity ring-down spectroscopy), optical HFOC (high-finesse optical cavity), and annular denuder equipped with online ion chromatography.

The average of all sites reached  $8.0 \pm 8.9 \mu\text{g m}^{-3}$ , with minimum and maximum of 0.2 and  $54.4 \mu\text{g m}^{-3}$ . The vast majority of the sites exceeded the UNECE Cle threshold of  $1 \mu\text{g m}^{-3}$  set for NH<sub>3</sub> to protect ecosystems and the  $3 \mu\text{g m}^{-3}$  threshold for other vegetation.

For the group of sites excluding FAHs (non-FAHs, Figure 4a and Figure 5), the mean concentration reached  $3.2 \pm 1.8 \mu\text{g/m}^3$ . For these non-FAH sites, the highest annual average concentrations,  $4.7 \pm 3.2$  and  $4.5 \pm 1.0 \mu\text{g/m}^3$ , were recorded at IND and TR sites,  $3.3 \pm 1.5$  and  $2.7 \pm 1.3 \mu\text{g/m}^3$  at UB and SUB sites, and  $1.0 \pm 0.3 \mu\text{g/m}^3$  at an RB site (Figure 7.2). Thus, NH<sub>3</sub> levels were higher at TR sites compared to UB sites, owing probably to NH<sub>3</sub> slip from vehicles. This possibility highlights the importance of considering the implementation of NH<sub>3</sub> emission limits for all times of vehicles. Thus, EURO 7 standard did not include an NH<sub>3</sub> limit value for passenger cars and vans, and for AQ it is very important that this emission limit value apply also to these vehicles, as for heavy-duty vehicles (EURO VI and VII). Furthermore, UB sites might receive NH<sub>3</sub> contributions from other sources, such as waste management and sewage systems that could also significantly impact urban NH<sub>3</sub> levels (Reche et al., 2012, 2015; Pandolfi et al., 2012). Therefore, in non-FAHs, IND, TR and UB sites urban sources are the main contributors to NH<sub>3</sub> ambient concentrations, and probably not always these are adequately accounted in the emission inventories.

When considering only FAHs (Figure 4.17), NH<sub>3</sub> concentrations were similar at SUB, RBCH, UB, TR sites ( $14\text{--}15 \mu\text{g/m}^3$ ), and  $10.0 \pm 2.3 \mu\text{g/m}^3$  at the IND sites. Thus, in this case, SUB and RBCH reached slightly higher NH<sub>3</sub> concentrations, probably because in these FAH sites, very large volumes of NH<sub>3</sub> are emitted by nearby agriculture and livestock (Sutton et al., 2022). Thus, UB-FAH NH<sub>3</sub> average concentration ( $14.0 \pm 5.3 \mu\text{g/m}^3$ ) was 4-fold higher than the one for UB-non-FAH sites ( $3.3 \pm 1.5 \mu\text{g/m}^3$ ).

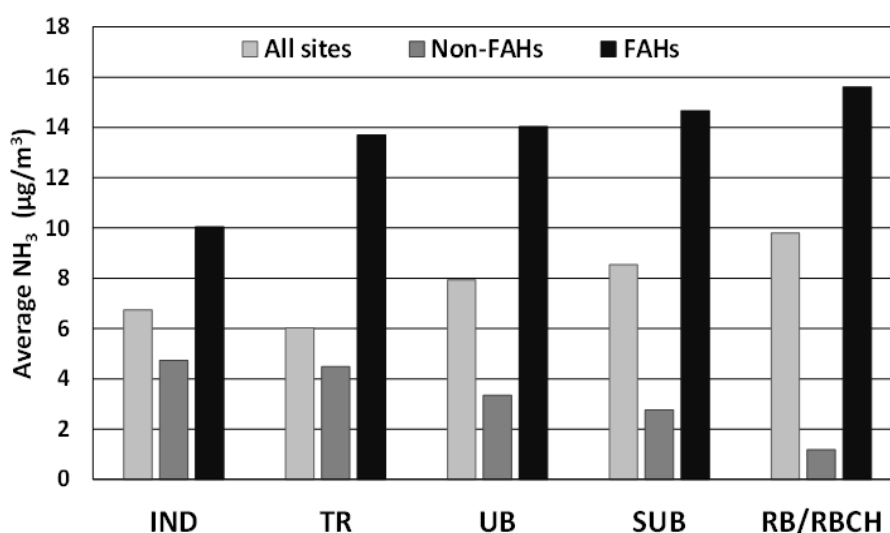


**Figure 4.17.** Average NH<sub>3</sub> concentrations for all (69) sites, outside (non-FAHs) and inside (FAHs) farming/agricultural hotspots, according to the type of environment: industry, IND; traffic, TR; urban background, UB; suburban background, SUB; regional background, RB, and regional background close to hotspots, RBCH. Figure modified from Liu et al. (2024a).

For the **non-FAHs sites**, the trend analysis showed the following results (Figure 4.18):

- Trends were very variable for the different sites in all types of environments (UB, TR, RB, IND) and this yielded to non-statistically significant trends in the analysis of each type, and for all types.
- Regarding UB and TR sites (N=7), three sites followed a statistically significant decreasing trend, while other three sites followed a statistically significant increasing trend.
- For the RB sites, a slight non-significant decreasing trend was observed.

For the **FAHs sites**, the trend analysis showed the following trends (Figure 4.18):

- A statistically significant decreasing trend was obtained at two of the UB sites (N=3, Figure 4), yielding to an overall non-statistically significant trend for all UB sites.
- For the RBCH sites, a statistically significant increasing trend was obtained for seven sites. Aas et al. (2024) attributed the NH<sub>3</sub> increasing trends of RB to their progressively decrease in the NH<sub>3</sub> consumption to generate (NH<sub>4</sub>)<sub>2</sub>SO<sub>4</sub> and NH<sub>4</sub>NO<sub>3</sub> associated with the marked decreases in the emissions of SO<sub>2</sub> and NO<sub>x</sub>. However, the articles referred to background NH<sub>3</sub> concentrations, while the RBCH sites (with extremely high NH<sub>3</sub> concentrations), were located in NH<sub>3</sub> FAHs, where an increase in emissions of this pollutant cannot be discarded in addition to the cause above.

It is important to consider these trends, with those on emissions and atmospheric processes to assess the current situations and to devise effective NH<sub>3</sub> abating policies.

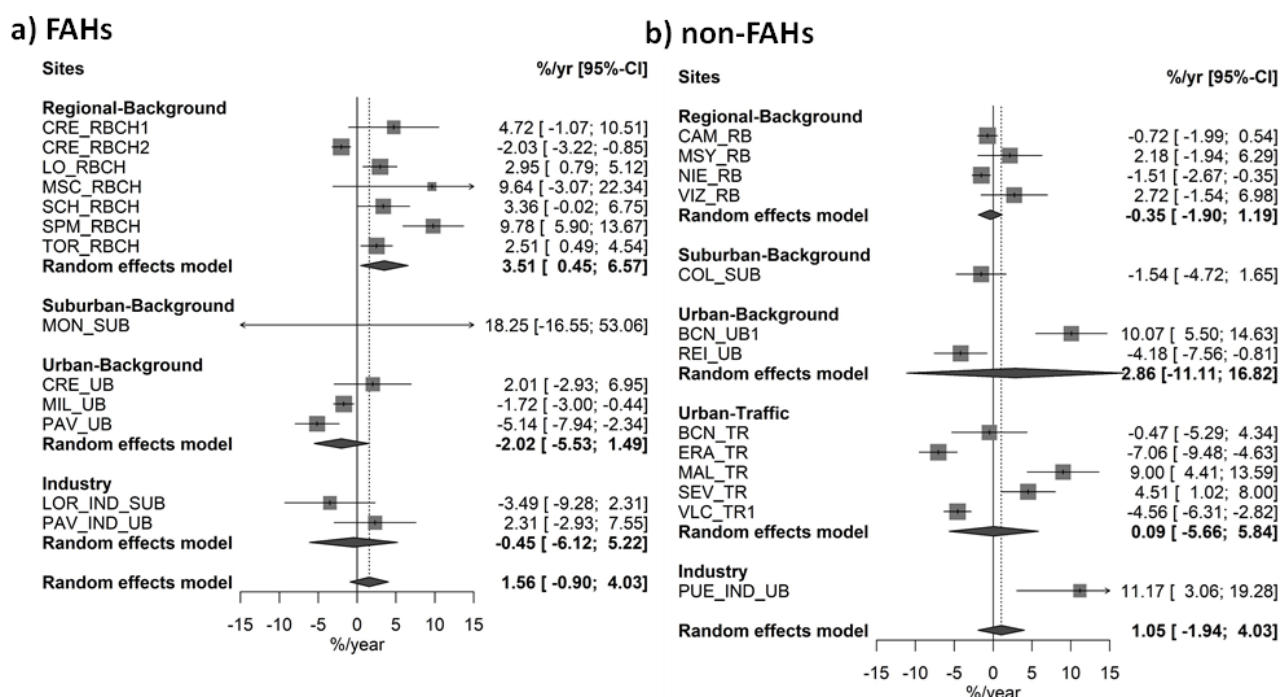


**Figure 4.18.** Annual NH<sub>3</sub> trends at (a) FAHs and (b) non-FAHs. Values represent change per year (%/yr) with 95% confidence level range in square brackets. Modified from [Liu et al. \(2024a\)](#).

#### 4.6. The added value of measuring VOCs in urban Europe

Based on the EU Directive 1999/13/EC of 11 March 1999, volatile organic compound (VOC) means any organic compound having an initial boiling point less than or equal to 250°C measured at a standard pressure of 101,3 kPa. VOCs exhibit a variety of functional groups and can be categorized by certain structural and reactive features, according to the way carbon bonds to itself or another element, e.g. carbon double bonded to oxygen. These different ways of bonding will lead to different reactivities with ambient oxidants (OH, NO<sub>3</sub>, O<sub>3</sub>). Table 4.3 presents the different families of VOCs based on their functional groups.

For benzene, three different reference methods are available (EN 14662-1-3). In addition, two other CEN standards (EN 14662-4-5) have been published that can be used for e.g. indicative measurements of benzene. For other VOCs, standardisation work is ongoing in the CEN working group TC264/WG13.

Typically, abundant compounds observed in ambient air and commonly reported in the literature include non-methane (NM) hydrogenated VOCs (HVOCs) such as alkanes (ethane, propane, and higher compounds), alkenes (ethylene, propene, etc.), aromatics (benzene, ethylbenzene, toluene, C<sub>8</sub>- and C<sub>9</sub>-aromatics, styrene), biogenic compounds (isoprene, monoterpenes, sesquiterpenes), and oxygenated VOCs (OVOCs) such as alcohols (methanol, ethanol, etc.), ketones (acetone, methyl ethyl ketone, etc.), aldehydes (formaldehyde, acetaldehyde, etc.), carboxylic acids (formic, acetic, etc.) and other families reported in Table 4.3. Terpenes are in general highly reactive and their oxidation leads, among others, to the formation of oxygenated VOC of various volatilities and chemical structures with different properties (reactivity, stickiness, etc.). OVOCs also play an active role in the chemical reactions chain of the atmosphere and are precursors of photochemical O<sub>3</sub> and SOA, as all the VOC chemical families. These compounds (OVOCs including formaldehyde, and terpenes) are among the recommended World Meteorological Organization (WMO) Global Atmosphere Watch (GAW) measurement variables (GAW-WMO, 2017). The measurement of these compounds is challenging due to their reactivity, as these compounds interact with surfaces, leading to possible artefacts during the sampling stage due to adsorption and desorption effects or to the ozonolysis of unsaturated VOCs in the sampling lines.

**Table 4.3.** Chemical families of VOCs.

Family	Molecular formula	Functional group (R=Alkyl group)
Alkanes	C <sub>n</sub> H <sub>2n+2</sub>	-C-C-
Alkenes	C <sub>n</sub> H <sub>2n</sub>	-C=C-
Alkynes	C <sub>n</sub> H <sub>2n-2</sub>	-C≡C-
Halocarbons	C <sub>n</sub> H <sub>2n+1</sub> X	-X: F, Cl, Br, I
Alcohols	C <sub>n</sub> H <sub>2n+2</sub> O	-OH
Ethers	C <sub>n</sub> H <sub>2n+2</sub> O	R-O-R
Aldehydes	C <sub>n</sub> H <sub>2n</sub> O	R-CH(O)
Ketones	C <sub>n</sub> H <sub>2n</sub> O	R-C(O)-R
Carboxylic acids	C <sub>n</sub> H <sub>2n</sub> O <sub>2</sub>	R-C(O)OH
Esters	C <sub>n</sub> H <sub>2n</sub> O <sub>2</sub>	R-C(O)-OR
Amines	C <sub>n</sub> H <sub>2n+1</sub> NH <sub>2</sub>	-NH <sub>2</sub>
Nitriles	C <sub>n</sub> H <sub>2n-1</sub> N	≡N

The VOCs list in Annex VII of the NAQD 2024/2881 include 45 VOCs from different chemical families including non-methane hydrogenated VOCs (NM hydrocarbons or HVOCs), OVOCs and terpenes. The NAQD mentions that measurement of O<sub>3</sub> precursors shall include at least nitrogen oxides (nitrogen monoxide NO and nitrogen dioxide NO<sub>2</sub>), and as appropriate, methane (CH<sub>4</sub>) and VOCs. The selection of the specific compounds to be measured will depend on the objective sought and may be completed by other compounds of interest.

The RI-URBANS/ACTRIS [ST5](#) on Measurements of VOCs supply guidance on the different techniques that might be used for measuring concentrations of the VOCs included in the NAQD, including chemical ionization mass spectrometry (CIMS), proton transfer mass spectrometry (PTR-MS), selected ion flow tube mass spectrometry (SIFT-MS), and atmospheric pressure interface CIMS (API-CIMS), together with chromatography associated with various detection methods. On the one hand, a technique using mass spectrometry can offer a very good temporal resolution (few seconds to few minutes) compared to gas chromatography (GC) and high-performance liquid chromatography (HPLC) techniques (1 h in general), but on the other hand these techniques are limited in the number of compounds that can be speciated. In contrast, GC techniques provide a better speciation for a large number of compounds at the expense of time resolution. These techniques have to be chosen depending on the application. The use of online instruments with a high temporal resolution is particularly useful in studies where probing fast processes is the main point of interest, such as emissions of pollutants and possible chemical reactions and/or transformations. Online GC and offline methodologies (i.e., HPLC, canister or tube sampling/offline analysis by GC) permit the measurement of a large pool of compounds with a time resolution ranging from 1 h to several days, which is of particular interest for SA, trend analysis or exposure studies. The NAQD indicates that Member States may use the method which is considered to be suitable for the monitoring objective sought, however, once available, standardised reference methods shall be applied. RI-URBANS guidance on tools to implement VOCs SA analyses are also available in [ST11](#).

#### 4.6.1. Emissions of VOCs

The current knowledge on VOCs origins as reviewed by the UK Air Quality Expert Group ([AQEG-UK, 2020](#)) is summarised here.

**VOCs from natural gas** production, distribution and use include methane, ethane, propane, butane. Many of them have a limited O<sub>3</sub> formation potential but should still be considered as significant O<sub>3</sub> precursors due to their high concentrations.

**VOCs from fuels** such as gasoline (production, distribution, engine emissions and evaporation) include i/n-butane and i/n-pentane, hexane, mono-aromatics (such as benzene, toluene, and m/p-xylene) and a fraction of unsaturated hydrocarbons (alkenes and alkynes). In recent decades, the amount of ethanol added to gasoline (up to 5–10%) has increased, while its content in PAHs (<30%), benzene (<1%) and di-enes (<1%) has been reduced to comply with the European standard EN 228 (2012 and A1:2017). In addition to these measures, the reduction of emissions by refineries, VOC traps at petrol stations, 3-way catalysts, together with the reduction in the use of direct petrol injection ([AQEG-UK, 2020](#)), have contributed to a very marked reduction in emissions from road transport and associated products. In addition to road traffic, benzene emissions can be partly attributed to off-road machinery, aviation, gas and biomass boilers, as well as forest fires and agricultural waste burning ([Lewis et al., 2013](#)).

**Solvent VOCs** include those emitted from industrial processes (manufacturing and application of paints and varnishes) to domestic use of products (personal hygiene, cleaning, adhesives, inks, paints, sealants, air fresheners and varnishes, among others). Species emitted by solvents include toluene, m,p,o-xylene, ethylbenzene, trimethylbenzenes, acetone, methanol, ethanol, isopropyl alcohol, formaldehyde, and halogenated alkanes

(dichloromethane, among others). The introduction of the European Commission Paints Directive 2004/42/EC may have had a major effect on reducing VOC emissions.

**Biogenic VOCs (BVOCs)** are isoprenoids that are emitted by wild and cultivated plants (e.g. isoprene in deciduous forests, and monoterpenes in evergreen forests). In addition to being emitted in large volumes during the summer in regions with high levels of sunlight, their potential for the formation of O<sub>3</sub> and secondary organic PM is very high. Although BVOC emissions are much lower than anthropogenic VOC (AVOCs) emissions on an annual basis, their relative importance is much greater during the critical O<sub>3</sub> pollution season. In addition, the spatial distribution of BVOCs and AVOCs (as well as NO<sub>x</sub>) emissions is different, and the former may determine the O<sub>3</sub> formation regime (controlled by the VOC/NO<sub>x</sub> ratio) across large areas.

Furthermore, a large proportion of VOCs in ambient air is of secondary origin, and they are generated from reactions such as ozonolysis and oxidation of hydrocarbons to OVOCs (aldehydes, ketones, among others). There are species such as formaldehyde that can have both primary and secondary origins, and some species that are both AVOCs and BVOCs. Thus, in regions with high solar radiation and O<sub>3</sub> concentrations, OVOC concentrations can be very high, due to their fast generation from primary HVOCs. In urban environments, OVOCs reach higher concentrations than the HVOCs normally measured by AQMNs.

#### 4.6.2. Concentrations of VOCs

In the framework of RI-URBANS, Liu et al. (2025b, under review) compiled 21 VOC datasets across mostly urban Europe, including Belgium (7 sites), Finland (2), France (7), Switzerland (1), Spain (1), and the UK (3). The dataset comprised 3 industrial (IND), 2 traffic (TR), 15 urban background (UB), and 1 suburban background (SUB) sites. Furthermore, Liu et al. (2025c) included an additional UB site in Greece in a study focusing on BTEX in urban Europe.

Measurements of VOCs were carried out using a variety of methodologies and instrumentation, because there is not a standard or reference method to this end. Accordingly, there is a limitation to data comparison due to the different protocols used for VOCs, but also because the disparity of VOCs species measured at each site. Furthermore, some of the techniques used are not able to trap specific VOCs for subsequent desorption and analysis, and other tools are not specific for a number of VOCs but for ions from a group of VOCs (such as in some cases for PTR-MS and specific groups). In this compilation, all monitoring stations monitored benzene since it is regulated, as well as toluene, ethylbenzene, and xylene species. However, none of the supersites yielding the 21 datasets cover all 45 VOCs of the NAQD 2024/2881. The studied sites included at most 29 VOCs while most of them measured more than 21 VOCs. This is reflecting the difficulty in measuring the 45 VOCs species.

It was observed that the 20 most commonly analysed VOCs at the monitoring sites were n-butane, n-pentane, i-pentane, n-hexane, n-heptane, n-octane, i-octane, 1,3-butadiene, 1-butene, trans-2-butene, cis-2-butene, 1-pentene, benzene, toluene, ethylbenzene, m,p-xylene, o-xylene, 1,2,4-trimethylbenzene, 1,3,5-trimethylbenzene, and isoprene.

For facilitating the comparison of these VOCs' datasets, the Maximum O<sub>3</sub> Formation Potential (MOFP) was calculated for each site by multiplying the Maximum Incremental Reactivity (MIR) of each species by its concentration at that site (Venecek et al., 2018). The secondary organic aerosol (SOA) Formation Potential (SOAP) was calculated in a similar manner, by multiplying VOC concentrations by the SOA yield (YSOA) of each species obtained from Gu et al. (2021). Average values for all sites and species included are ranked in Figure 4.19.

The results evidenced that toluene, m,p-xylene, 1-butene, n-butane, and isopentane collectively contributed on average over 50% to the total MOFP (calculated as the sum of the individual 20 MOFPs) for the sites studied, with individual contributions of 15% ± 9%, 13% ± 7%, 9% ± 8%, 9% ± 6%, and 7% ± 5%, respectively. This is primarily attributed to their relatively high concentrations and high MIR values. In parallel, aromatic hydrocarbons accounted

for most of the SOAP (>85%), with toluene (55% ± 16%), benzene (20% ± 10%), m,p-xylene (7% ± 3%), and o-xylene (4% ± 2%) being the major contributors.

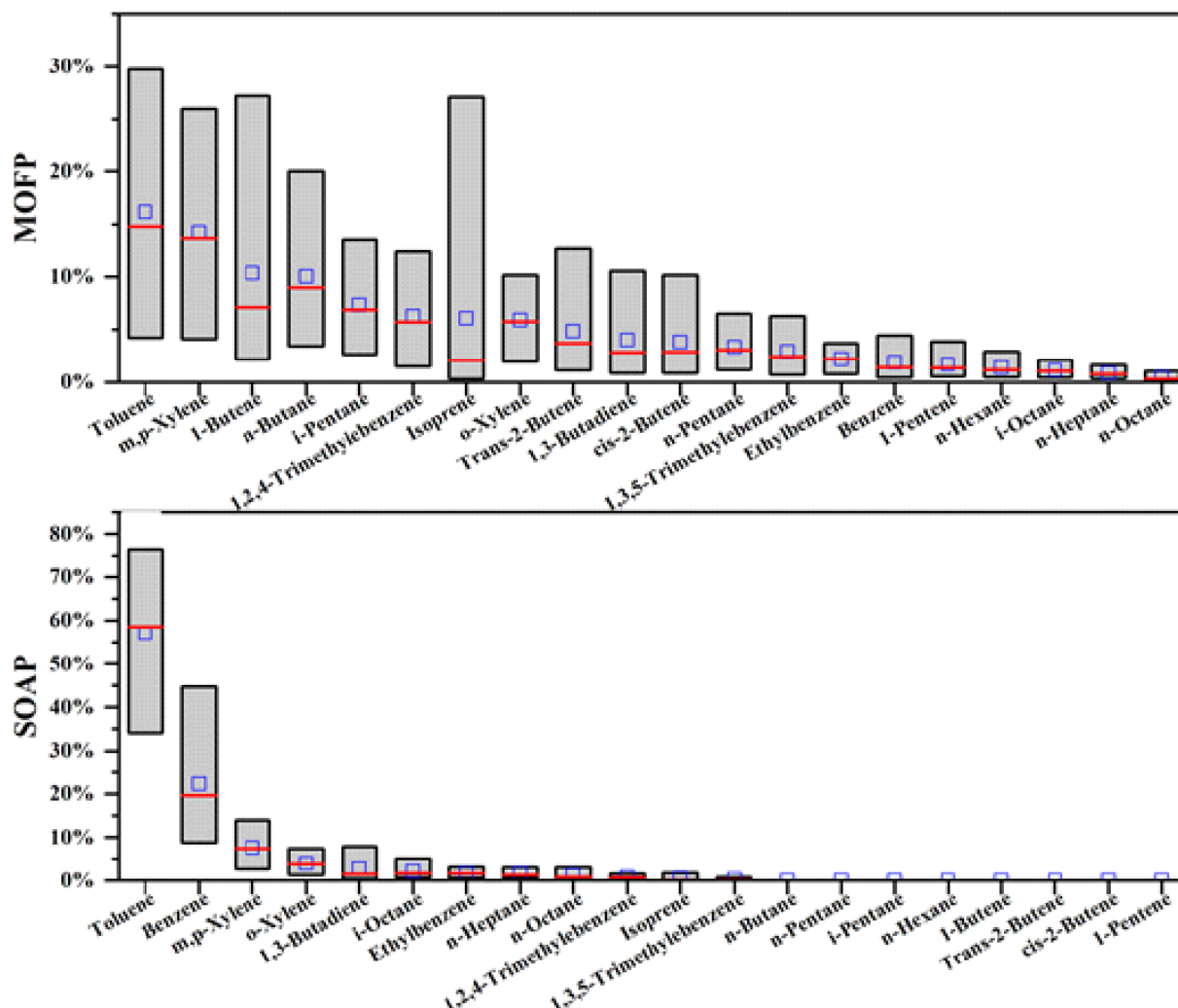


**Figure 4.19.** Individual contributions of 20 VOCs to (lower) the total (sum of the 20) SOA formation potential (SOAP), in  $\mu\text{g SOA}/\text{m}^3$  and (upper) the maximum O<sub>3</sub> formation potential (MOFP), in  $\mu\text{g O}_3/\text{m}^3$ , as averages for the collected datasets. The box represented the 5th–95th percentiles of ratios. The middle line and middle square represented the median values and mean values of ratios, respectively. Adopted from Liu et al. (2025b, under review).

Liu et al. (2025c) reported that BTEX can be ranked according to their 2017–2022 average concentrations as toluene > benzene > m,p-xylene > o-xylene > ethylbenzene, with mean concentrations of  $1.5 \pm 1.7$ ,  $0.8 \pm 1.0$ ,  $1.0 \pm 1.3$ ,  $0.4 \pm 0.5$ , and  $0.3 \pm 0.5 \mu\text{g}/\text{m}^3$ , respectively. Figure 4.20 shows the average concentrations observed at each site.

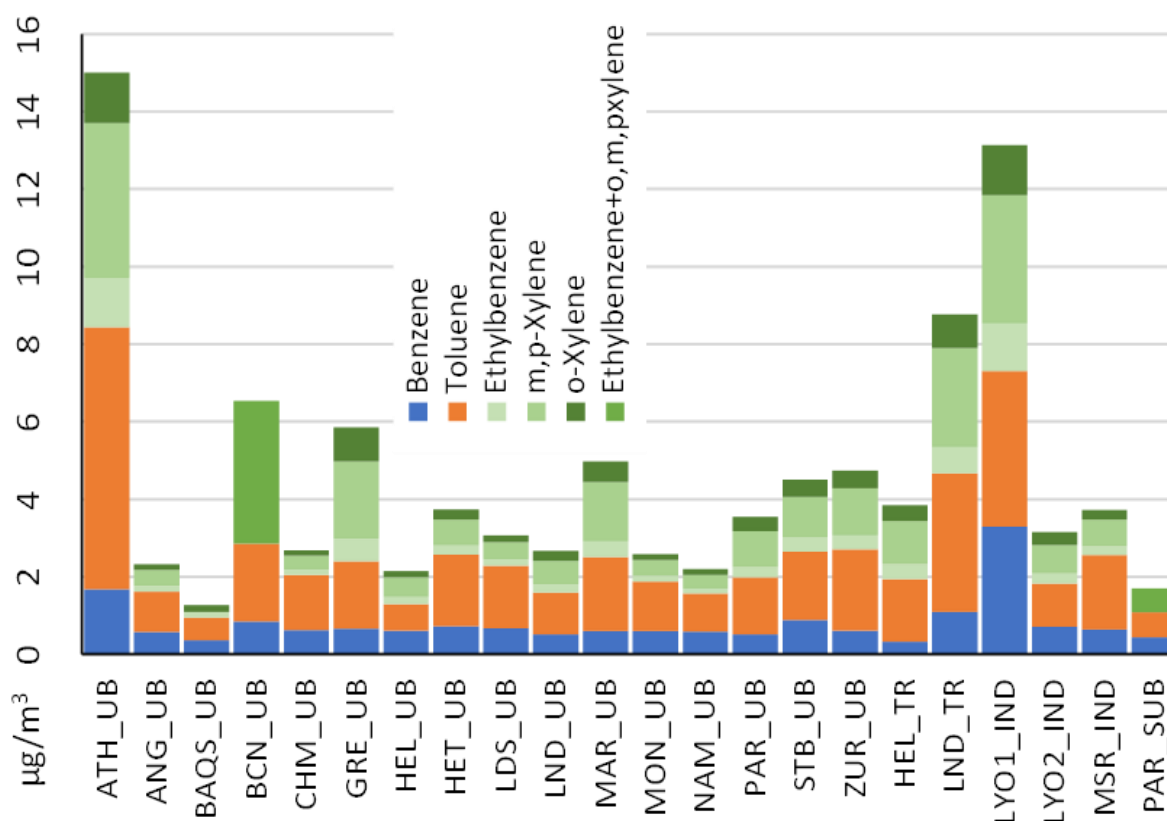


**Figure 4.20.** Average 2017–2022 concentrations for specific BTEX in the 22 study sites. The abbreviations stand for the following European cities: ATH for Athens, ANG for Angleur, BAQS for Birmingham, BCN for Barcelona, CHM for Charleroi, GRE for Grenoble, HEL for Helsinki, HET for Herstal, LDS for Lodelinsart, LND for London, LYO1 for Lyon (Feuzin stade), LYO2 for Lyon (Vernaison), MAR for Marseille, MON for Mons, MSR for Mouscron, NAM for Namur, PAR for Paris, STB for Strasbourg, and ZUR for Zürich. Modified from [Liu et al. \(2025c\)](#).

#### 4.6.3. Source apportionment studies of volatile organic compounds in Europe

The literature review on the SA of VOCs in UB and SUB sites showed that, to our knowledge, 18 studies have been performed in Europe. PMF receptor modelling was used in most of the cases to perform the SA either on seasonal basis when long term data is available, or on specific campaign's data. PMF with EPA 5.0 software is the most suitable as it does not require previous knowledge on the source composition profile.

A variety of sources were identified (some in some specific periods, such as biomass burning in winter) in the urban environment, which are described with their common tracers/markers below.

- Natural gas source was mostly identified by high contributions of ethane and propane, with minor contributions from butane.
- Wood-burning source was traced by acetonitrile, acetylene, ethylene, and benzene.
- The biogenic source was identified by isoprene and its oxidation products (methyl vinyl ketone (MVK) and methacrolein (MACR)). Although isoprene has a biogenic origin, its anthropogenic origin is rarely described. The addition of monoterpenes can potentially aid in identifying its biogenic origin, although they are often emitted

from other vegetation (potentially being identified as a separate factor), and also monoterpenes can be emitted from anthropogenic sources.

- Motor vehicle exhaust was characterized by high contributions from C4–C5 alkanes, especially butane and pentane, and BTEX (benzene, toluene, ethylbenzene, and xylenes) compounds. The exact tracers highly depend on the type of traffic and engines most commonly used in the urban area, and depending on the VOCs included in the study. The traffic exhaust was either separated or combined with fuel evaporation related to traffic.
- Solvent source markers often had high contributions of OVOCs and aromatics in these studies.
- Some specific industry sources were found, but this highly depended on the type of industry and on which VOCs were used to identify this source.
- Various studies found a secondary source composed of OVOCs mainly, although some studies identified this source as long-lifetime VOCs.

Within RI-URBANS, three SA studies were performed after data collection at two urban/urban background sites with different VOC datasets in Marseille, France ([Dufresne, 2022](#)), Zurich, Switzerland, and Barcelona Spain ([in 't Veld et al., 2023b](#)). As an example, Figure 4.21 shows the results of the PMF SA for Marseille and Zurich. These have some common VOC sources, such as road traffic, natural gas, heating/wood burning, and other local emissions (one source related to solvent use was identified only in Zurich due to OVOC that were measured, and additional sources in Marseille related to industrial sources). Since the two datasets did not cover the same VOCs, having a wide range of VOCs with varying volatility, including both primary NMHVOCs and secondary origins (OVOCs), is essential. This broader spectrum can aid in identifying the sources and assessing their contribution. Additionally, the measurement of OVOCs is important as it is an indicator of the impact of photochemistry and covers some markers of solvent use emission source.

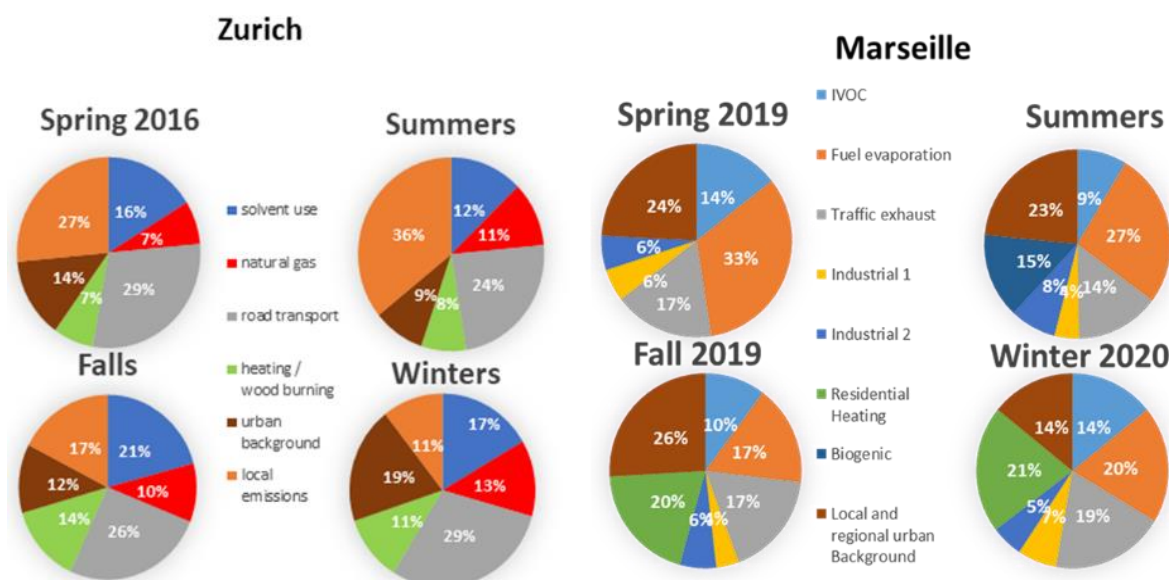


Figure 4.21. Source apportionment results at Marseille ([Dufresne, 2022](#)) and Zurich.

#### 4.7. Added value of measuring vertical profiles

Although measurements of vertical profiles of advanced AQ parameters are not required or recommended in the NAQD 2024/2881, the RI-URBANS, ACTRIS and IAGOS demonstrated that these are very useful for an advanced AQ assessment, forecast and validation of modelling tools.

RI-URBANS has produced three STs on vertical profiles in collaboration with ACTRIS or IAGOS. Thus, [ST7](#) contains guidance on measurements that allow to determine the atmospheric boundary layer (ABL) height (ABLH), a key parameter for forecasting, for example, exceedances of daily and hourly limit values; and [ST8](#) on aerosol profiles, which are very useful for detecting and demonstrating desert dust outbreaks, long transport of PM from anthropogenic or forest fires, over European cities. Finally, [ST9](#) shows the products from IAGOS on vertical profiles of AQ pollutants (NO<sub>2</sub>, O<sub>3</sub>, etc.) measured in commercial aircrafts and that can be openly accessed in the IAGOS website.

We provide here some examples on the added value of implementing these STs.

##### 4.7.1. Atmospheric boundary layer

The ABL is the lowest part of the atmosphere that is directly affected by the Earth's surface at time scales of <24 h. When the ABL is not well mixed, which may frequently be the case during the day-night transition and several hours around those times, multiple sublayers can have distinctly different composition characteristics. In clear sky conditions, buoyant mixing during the day dilutes pollutants within the so-called convective boundary layer (CBL) that increases in height during the morning and decays around sunset. At night, the vertical buoyancy is absent or weak, leading to a relatively shallow nocturnal layer close to the ground. The air diluted within the daytime CBL remains aloft and forms the residual layer. The height of the total atmospheric boundary layer (ABLH) represents the height of the residual layer at night and during morning while the CBL extends over the entire ABL in the afternoon. To define the volume for pollution dispersion and distribution near the ground, the continuum of the shallow nocturnal layer and the daytime CBL can be considered as the mixed layer height (MLH). The cloud-topped ABL can generate its own turbulent mixing which may be sufficient for a deep MLH to persist whether day or night.

Transport processes in the ABL can significantly affect the spatial distribution (horizontal and vertical) of aerosols and trace gases. While the horizontal wind is an important variable that drives horizontal advection between neighbourhoods or between the city and its surroundings, atmospheric turbulence is responsible for the mixing of the atmosphere, the vertical dilution of pollutants as well as the potential entrainment into the CBL. If fresh air is entrained, this can improve near-surface AQ, while entrainment of residual layer air or pollutants from elevated aerosol layers (e.g. Saharan dust, forest fire plumes) may have negative effects.

[ST7](#) guides on how to characterise the above parameters of the ABL using measurements with automatic lidars and ceilometers (ALC), and Doppler wind lidars (DWL). As an example, results are shown here for long-term MLH measurements by the ABL testbed project at the RI-URBANS pilot cities. The variability of ABL dynamics can be assessed at different temporal scales, from diurnal cycles to monthly or seasonal variations to inter-annual differences. As an example, the ABL testbed demonstrator project is currently processing data from 17 measurement sites (21 ALC) across Europe, including several sites relevant to RI-URBANS pilot cities: Bucharest (2 sites), Helsinki (2 sites), Aosta - St Christophe that is influenced by Milan (1 site), Paris (2 sites), and Rotterdam (2 sites), with daily quick looks freely accessible (ABL testbed – European: <https://observations.ipsl.fr/aeris/e-profile/>). Multiple years of measurements have been processed by the ABL testbed spanning from 2018–present for most sensors. Figure 4.22 shows an example of the MLH daily variability in Paris.

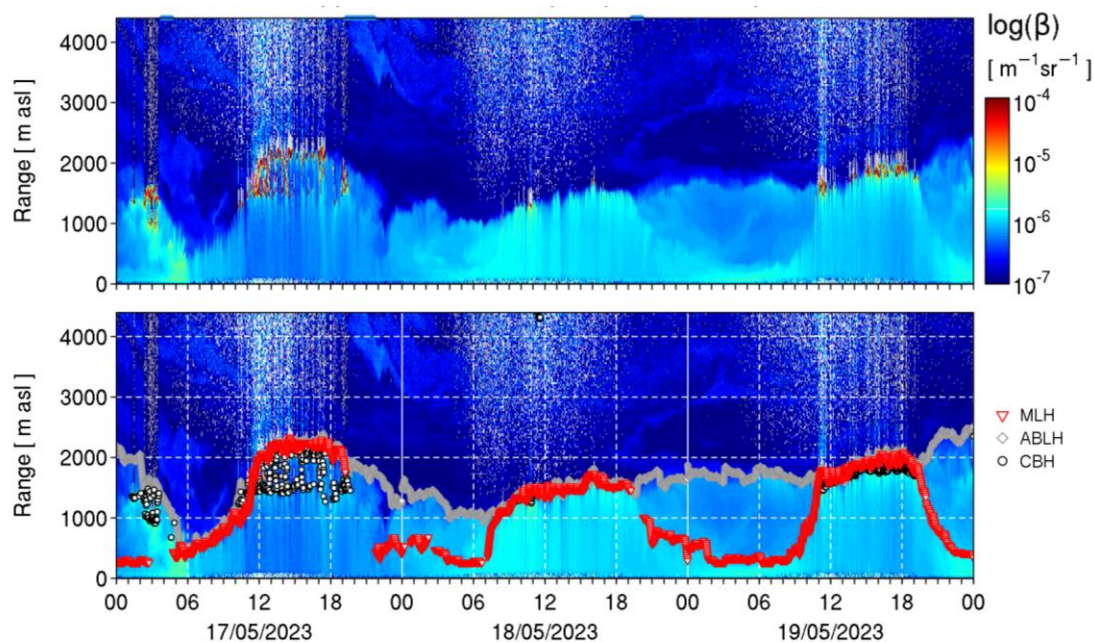


**Figure 4.22.** Daily quick look from the ABL testbed: overlap-corrected and calibrated attenuated backscatter observed with an ALC (Lufft CHM15k) at the SIRTA observatory at Palaiseau near Paris over a three-day period. Bottom figure also shows the cloud base height (CBH) and the mixed layer height (MLH) and atmospheric boundary layer height (ABLH) detected with the STRATfinder algorithm.

#### 4.7.2. Vertical profiles of aerosols

Surface based remote sensing measurements can yield to vertical profiles of the variation of the aerosol concentrations. These measurements coupled with the ones of the ABL can be very useful to detect long range-transport of PM (including dust, forest fires, anthropogenic pollution) and to evaluate the impact on surface levels by the growth of the MLH.

Aerosol profiling quantities are typically measured through range-resolved optical remote sensing, so that optical properties are the quantities measured and are typically dependent on the chemical composition and shape of the particles and on their concentration (e.g. aerosol extinction coefficient profiles). Some intensive parameters can then be directly obtained (typically through calibrated ratio of optical properties, e.g. depolarization ratio). Finally, some quantities can be retrieved from the previous quantities, such as the mass concentration.

Aerosol properties (known as quantities) measured are aerosol backscatter, aerosol extinction, volume depolarization ratio, among others. From these, the following intensive properties are obtained: lidar ratio, Angstrom exponent, backscatter Angstrom exponent, particle linear depolarization ratio, and aerosol type, among others.

As an example, results on the aerosol optical properties climatology over Europe 2000–2019 is shown. This study is based on EARLINET long term observations performed in 2000–2019, namely the Level 3 climatological products (EARLINET Level 3 Data Product Catalogue, 2022). In the following, examples for stations identified as of interest for urban conditions considering their population in the area are reported, and compared to stations in clean conditions to be considered as a reference/background. As representative of urban conditions, the following stations are reported: Madrid (ES), Barcelona (ES), Ispra (IT), Naples (IT), Athens (GR), Thessaloniki (GR), Warsaw

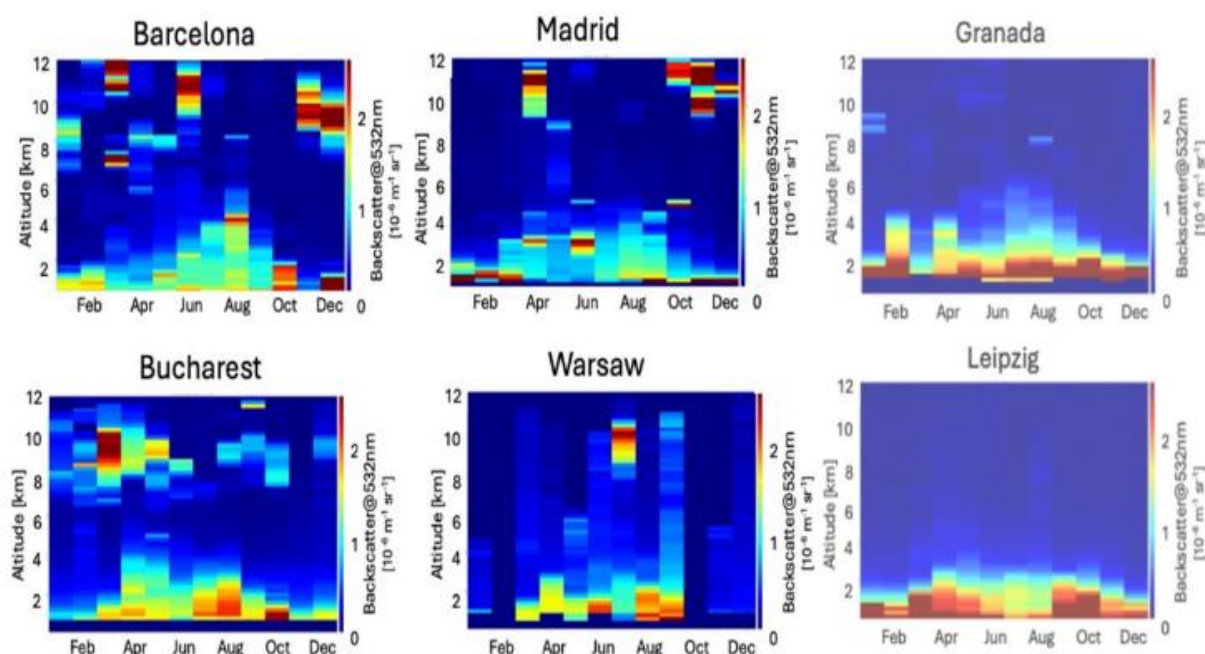
(PL), and Bucharest (RO). As reference for clean conditions, Granada (ES), Leipzig (DE) and Lecce (IT) stations are also reported.

Figure 4.23 reports normal months average profiles at 532 nm for each station, showing the seasonal dependence as observed during the last 20 years and relative differences between the stations. The false colour images of backscatter coefficient provide a direct insight of the presence in the atmospheric column of the aerosol particles: warm colours indicate the presence of high aerosol concentrations, while cold ones are for lower concentrations, until reaching the blue where the aerosol concentration can be considered below the detection limit.

Apart from signatures of aerosol presence above 6 km, due to special events of long range transported aerosol particles, most of the aerosol content is confined up to 4–5 km of altitude. The presence of aerosol up to higher altitude during warm periods is common to all the reported sites. Anyhow, it is observed a tendency of more pronounced trapping of aerosol closer to the surface at big cities locations (first two columns). This is clearly evident in the case of Naples, a metropolitan area located close to sea. Comparing the false colour maps in Figure 9.2 with the corresponding Lecce one (smaller city on the sea) it is clear the presence of intense red area close to ground for Naples while the yellow dominates with different nuances for Lecce, even if all the 3 show the same general pattern with higher altitude affected by aerosol in June–August period.

The same behaviour is observed for Iberian region (Barcelona and Madrid compared to Granada) and for central-East Europe (Bucharest and Warsaw vs. Leipzig). To be noted that the high aerosol content observed over Granada is probably related to the considerable presence of dust being in a very arid region and strongly affected by desert dust.

Thus, these measurements coupled with the ones of the ABL can be very useful to detect long range transport of PM (including dust, forest fires, anthropogenic pollution) and to evaluate the impact on surface levels by the growth of the MLH.



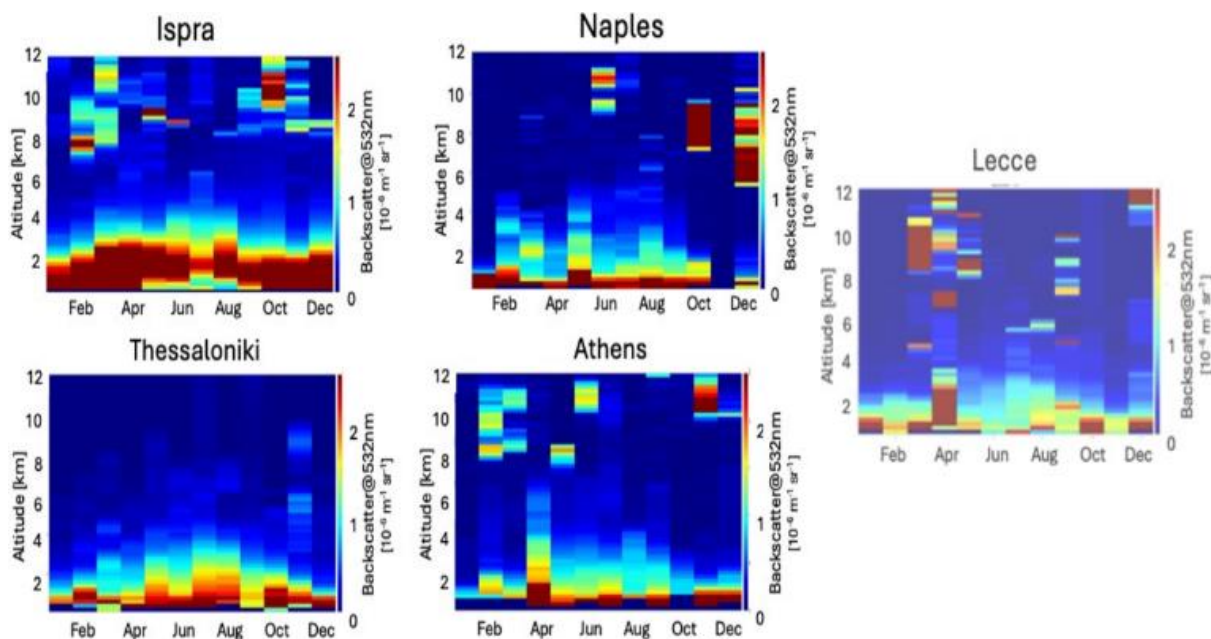


**Figure 4.23.** Climatological monthly averages of the aerosol backscatter profile at 532 nm in suburban locations close to eight big cities: Barcelona, Madrid, Bucharest, Warsaw, Ispra, Naples, Thessaloniki and Athens. In the third column the same quantity is reported, as partially transparent, for three sites far from big cities located in the same macro-area of the previously reported eight sites.

#### 4.7.3. IAGOS vertical profiles of pollutants

Using compact and automated in-situ sensors on board of passenger aircraft, the European RI IAGOS ([Petzold et al., 2015](#), [Thouret et al., 2022](#); [www.iagos.org](http://www.iagos.org)) monitors vertical profiles of trace gas concentrations (incl. CO, O<sub>3</sub>, NO<sub>x</sub>, and H<sub>2</sub>O) near airports during take-off and climb-out as well as during descent and landing flight phases between the ground and 10–12 km altitude. These profiles characterise the vertical distribution of trace gases from the free troposphere down to the regional-scale and urban background boundary layer that interacts with the urban pollution layer. In addition, elevated layers of polluted air that are often advected via regional or long-range transport can be identified with the help of IAGOS profiles and are assessed for their impact on urban AQ.

The IAGOS profile data provide valuable information that is otherwise not accessible, and complement the data provided by surface-based AQMN stations ([Petetin et al., 2018](#)), facilitating the link to high-resolution models and satellite observations particularly in the vertical dimension. Above the planetary boundary layer, the correlation between the IAGOS in-situ and the urban background observations decreases rapidly, while increasingly high correlations with remote Global Atmosphere Watch (GAW) stations. The representativeness of the IAGOS airborne measurements for the general conditions of the lower troposphere are carefully analysed by [Petetin et al. \(2018\)](#).

In the middle of 2024, IAGOS counted a fleet of ten aircraft equipped with automatic instruments operated by eight international airlines. Of these, six regularly sample the European troposphere with ozone and CO since 2002 and two of them provide additional NO<sub>x</sub> data since 2015 and 2023, respectively. A third one providing NO<sub>x</sub> is planned for the end of 2024. Thanks to several equipped aircraft landing or taking off over the same airport, it may be possible to access the diurnal cycle of those parameters, as has been shown for O<sub>3</sub> in [Petetin et al. \(2016\)](#).

A visualisation service is available at [www.iagos.org/products](http://www.iagos.org/products). This service displays the most recent profiles at worldwide airports as compared with the Copernicus Atmosphere Monitoring Service (CAMS) models on both

global and regional scales. A subset of profiles over the RI-URBANS pilot cities is accessible under the category RI-URBANS (see Figure 4.24). Currently, the pilot cities available are Milano, Barcelona, Paris, and Zurich. In the first instance, they are compared with the CAMS global models, but will soon include the CAMS European AQ models on the regional scale. At the time of writing this guidance, profiles available are for O<sub>3</sub> and CO and a similar service is under development for NO<sub>x</sub>.

Figure 4.24 also illustrates the vertical profile of O<sub>3</sub> as observed over Barcelona during the morning profile (a) with around 15 ppb of O<sub>3</sub> at the surface and the second profile b) with and around 55 ppb by noon.

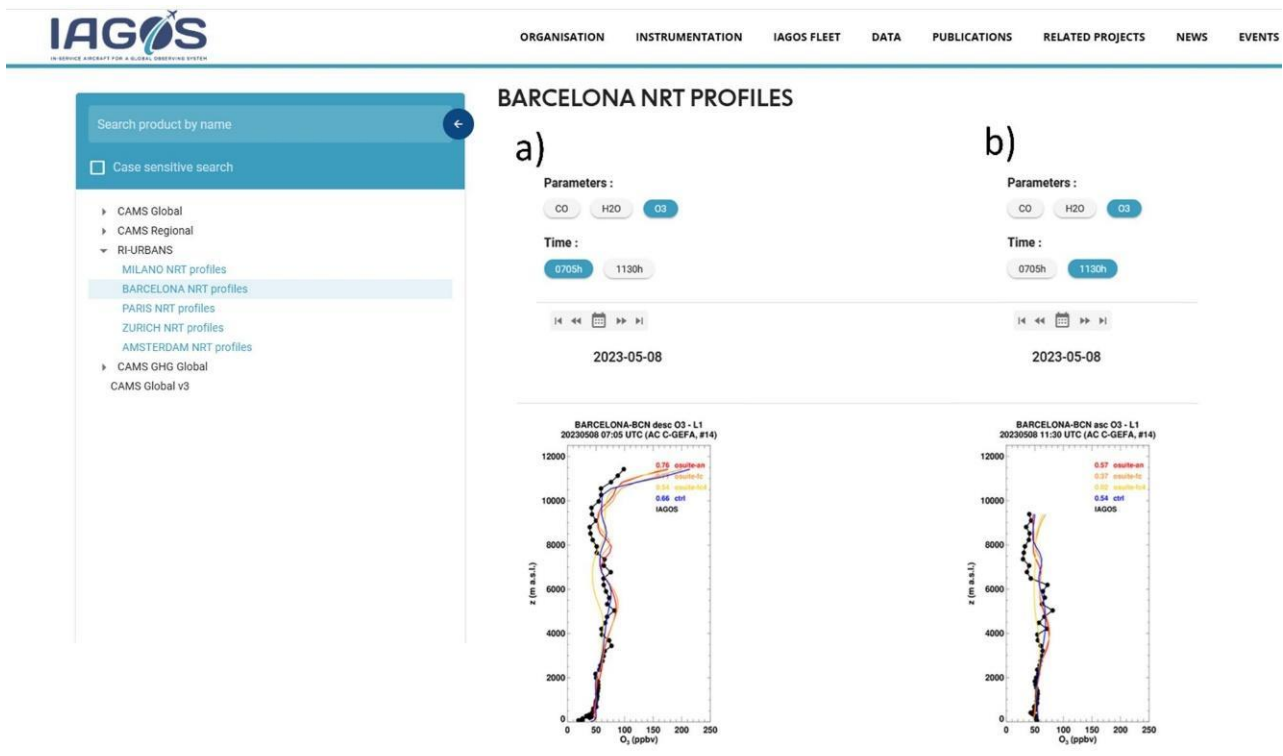


**Figure 4.24.** Combined screenshots of the visualisation service for profiles (available at [www.iagos.org/products](http://www.iagos.org/products)) over Barcelona. The diurnal O<sub>3</sub> profile as observed during the morning (a) and around noon (b).

## 4.8. Added values of urban mapping and citizen science

Spatial mapping of novel AQ pollutants in urban areas can be done by using fixed and/or mobile measurements and by different types of modelling approaches. In RI-URBANS, the suggested urban mapping approaches are summarised in [ST12](#) (on deterministic modelling for mapping PM and UFP at urban scale), [ST13](#) (on mapping UFP and citizen science), and [ST16](#) (on mapping UFP using multiscale modelling approaches). The approach suggested by [ST12](#) and [ST16](#) has been commented on in the chapter on UFP-PNSD of this document. In this section only mapping according to ST13 recommendations are reviewed.

### 4.8.1. Mapping of novel AQ parameters

Different approaches can be used to assess urban variability of ambient concentrations of AQ pollutants at high spatial resolution for epidemiological studies and other applications. Mobile sensing platforms (equipped with high-, middle or low-cost sensors) and fixed (low-cost) sensor networks can be used as complementary tools to data from fixed regulatory AQMNs to map pollutant concentrations at a higher spatial density.

A distinction between mobile/fixed measurements and experimental designs with/without citizens, has been made in [ST13](#). The collected data can be processed and analysed using only measured data or using interpolation/modelling techniques like Land Use Regression (LUR)-based or machine learning models. The selected techniques used for data processing may have an impact on the required data collection approach. Each of the approaches has strengths and weaknesses. When selecting a method, the user needs to define the aim of the data collection and other considerations e.g. one may prefer to engage citizens as part of awareness training on AQ (Figure 4.25). Deliverables [D13](#) and [D14](#) from RI-URBANS show in more detail the methodologies and examples of mapping exercises done in the project (two examples are shown below).

Mobile monitoring can be used to map pollutants at a high spatial resolution with a limited number of instruments (in contrast to stationary monitoring) and can also use high-end or mid-end instruments exhibiting higher data quality than sensors. Mobile monitoring has some challenges because of the spatiotemporal nature of the collected dataset. Care should be taken during data collection and/or data processing in order to obtain representative results.

Low-cost fixed sensor networks have several limitations, especially for the real-time sensors which have shown varying performances. Good performance has been documented for low-cost diffusive (or passive) samplers. Diffusive samplers only provide weekly to monthly averages, but this may be sufficient for specific use cases. If so, diffusive samplers are the method of choice. While real-time sensors are able to provide very frequent measurements, they lack the accuracy of the substantially more expensive regulatory grade instruments and are greatly affected by extreme meteorological conditions (mainly high relative humidity). Therefore, a proper calibration and validation approach is needed. We recommend co-location performance evaluation to evaluate intra- and inter-sensor uncertainty and continuous calibration/validation under representative pollutant and meteorological conditions to compensate for seasonal effects from e.g. temperature and relative humidity. Regardless of that, they provide sensing opportunities that were not feasible before due to their portability and low cost. Using a spatially dense network can help in measuring and understanding the effect of sources that are usually “lost in the big picture”, such as the effect of hyper-local sources of pollution.

Figure 4.26 shows an example of the urban mapping of the concentrations of UFP using mobile platforms and coupling these with LUR modelling for the city of Bucharest.

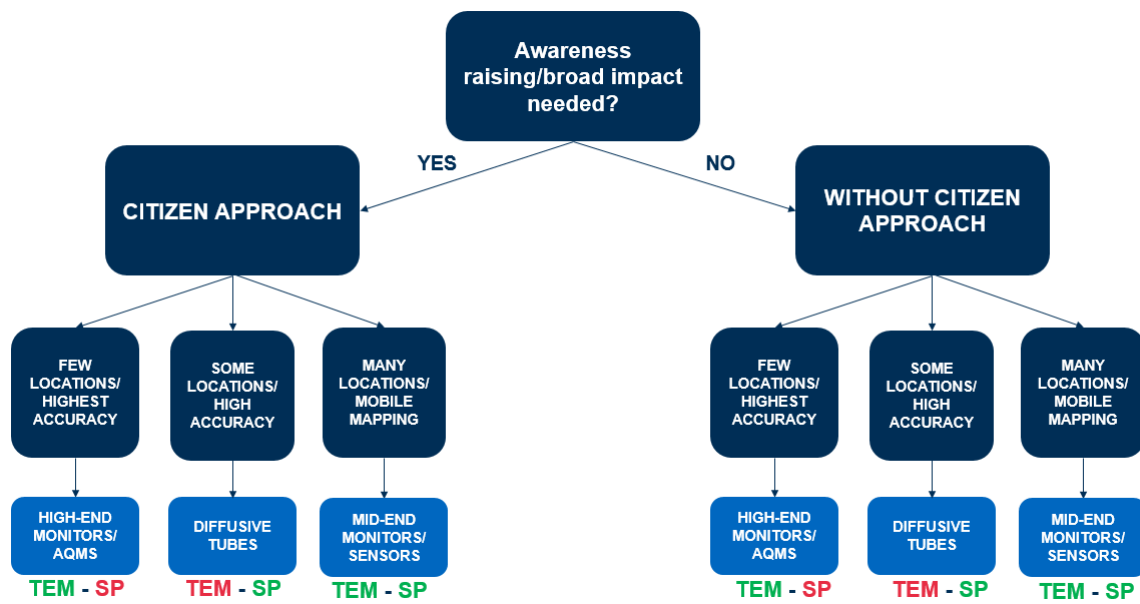


Figure 4.25. Pathways for selecting methods for urban mapping. TEM refers to temporal and SP to spatial. Green implies that the method performs well, red that it performs poorly for the spatial or temporal aspect.

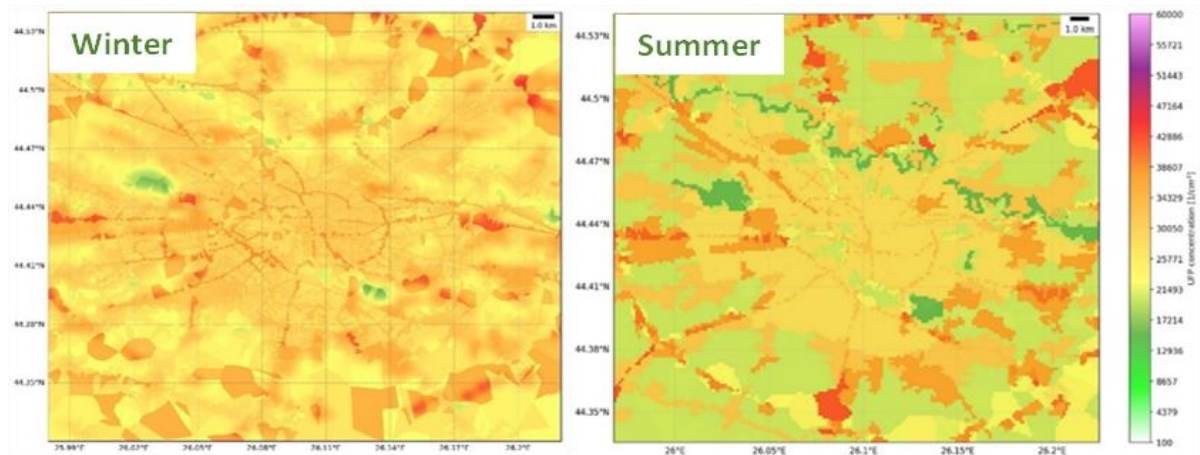


Figure 4.26. Model-measurement maps of UFP concentrations in Bucharest during winter and summer.

Overall conclusions are:

- Mobile monitoring can collect more datapoints but gives a snap-shot (no time trends). Repeated measurements, and associated sensitivity analysis, are needed to obtain representative results.
- Post-processing (data cleaning, rescaling) and model approaches have shown to be viable approaches to translate mobile measurements into actionable long-term exposure data.
- Mobile monitoring can be performed by repeating predefined fixed routes or using a more opportunistic approach, using a carrier that performs the measurements during its day-to-day activities without intervening with these activities.

- Targeted mobile monitoring makes it easier to compare different locations compared to opportunistic approaches, but are often more constrained in space and time.
- Opportunistic approaches mostly require less effort in data collection, result in large datasets but need proper processing to obtain representative results.
- Involving citizens can significantly contribute to awareness raising and obtain impact from the collected results, but will require more time and effort for communication, logistics and dissemination.
- Sensors can be deployed at a lower cost compared to mid- and high-end instruments but suffer from lower data quality. If a high temporal resolution is no requirement, diffusion samplers may be the preferred low-cost approach.
- Sensor calibration and compensation can significantly improve data quality.
- Different approaches for sensor calibration are used, varying from co-location calibrations with reference methods, or purely data-driven models including known covariates (e.g. temp, RH, O<sub>3</sub>).

#### 4.8.2. Mapping and involvement of citizen science

In RI-URBANS, the citizen science approach is summarised in **ST13** (Mapping UFP and citizen science). This approach can raise awareness of the urban citizens to air pollution issues. The **ST13** provides a comprehensive guidance on motivating the citizens to take part in AQ monitoring and provides best practices and recommendations. It further elaborates the added value of complementing stationary sensor networks with mobile measurements and provides analysis of the lessons-learned from the RI-URBANS pilot studies.

The NAQD (2024/2881) on ambient AQ and cleaner air for Europe connects to the European Union's objective towards zero pollution by 2050 facilitating a marked abatement of premature deaths due to air pollution. The NAQD merges the 2004 and 2008 legislation and responds to the recommendations from the WHO AQ Guidelines and to monitor additional air pollutants, such as UFP, PNC, NH<sub>3</sub>, and BC concentrations. The European Member States have two years to transpose the requirements of the NAQD. The NAQD is aligned with “The European Green Deal”, which is an ambitious roadmap towards resource-efficient and competitive European society, which protects the well-being of the citizens e.g. from negative health impacts caused by poor AQ.

The EU set up stricter AQ standards and expanded the network of AQ observations, including the AQ supersite concept as well as separate requirements for the member countries to quantify the importance of air pollution hotspots. The NAQD further requires improved public involvement with informing the citizens about the AQ issues and their health implications and encourages and empowers community participation in AQ improvement efforts.

The added value of citizen observations comes from the capacity to supplement the official monitoring. The citizens can contribute e.g., by operating low-cost sensors to measure local AQ in their local neighbourhood, which increases spatial coverage and can identify pollution hotspots. These data can complement official AQMNs, filling gaps in areas lacking sufficient coverage. A specific weight should be placed on quality control of the data, for example allowing side-by-side measurements in official AQ monitoring sites, when applicable and feasible. Figure 4.27 shows, as an example, the mapping of the concentrations of BC in Rotterdam using mobile measurements with citizen involvement.

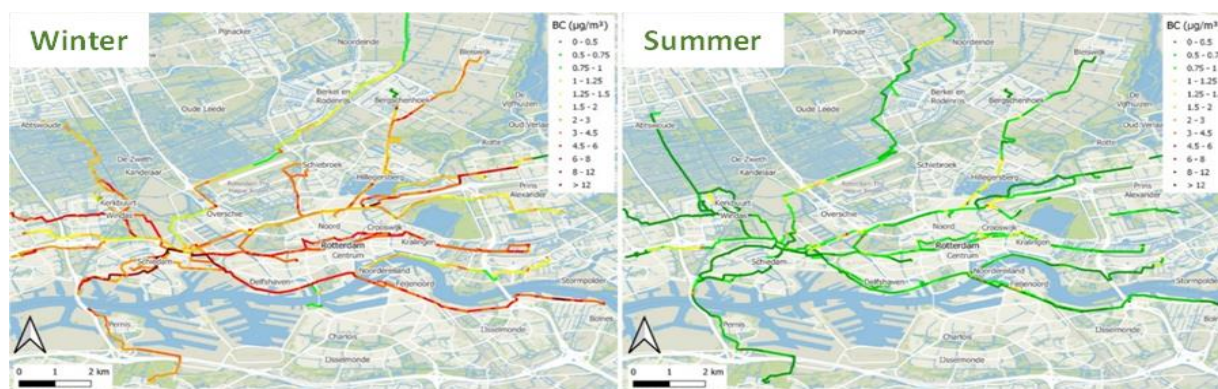


**Figure 4.27.** Average BC concentrations ( $\mu\text{g}/\text{m}^3$ ) from mobile monitoring involving citizens in Rotterdam.

The citizen science activities foster awareness of pollution levels and its health impacts. This can drive personal behavioural changes, such as reduced car use or reduced waste burning. At the same time, citizen involvement empowers local communities as a whole. The citizen-generated data can empower communities to hold governments accountable for meeting AQ standards enabling grassroots movements to advocate for cleaner transportation, industry regulations, or urban greening. Citizen science should be connected to data validation and collaborative scientific activities with AQ experts. In an ideal case, citizen science projects can work alongside researchers and policymakers for example to validate AQ models or to evaluate the impact of a specific AQ measure. The collaboration with AQ scientists supports that the citizen-generated data meets scientific standards for reliability and usability.

In summary, citizen involvement in AQ monitoring supports AQ policy implementation by connecting the urban citizens with the decision makers in local, regional and national levels. This facilitates transparency of AQ policies. The citizen science projects can help policymakers fine-tune local strategies by providing hyper-local data that complements official AQMNs. The new data can lead to behavioural change in individual and community levels while allowing grassroots participation and sense of influencing steps towards cleaner air, improved public health, and a more engaged society.

## 5. FINAL CONSIDERATIONS

Concentrations of most AQ pollutants decreased markedly in urban Europe during the last 20 years as a consequence of the European, national, regional and local AQ policies implemented since the first AQ EU Directive (1996/62/EC). Specific AQ directives, such as the ones on Industrial Emissions, Large and Medium Scale Combustion Plans and the ones fixing EURO emission standards for vehicles, among others, had a high impact in abating AQ pollutants. National and regional actions took place to implement these directives, as well as additional policies. At the local scale, low emission zones, congestion charges, policies on domestic sources, among others, contributed also to abate pollution in urban areas. These marked decreases of pollutants were reached mostly by reducing emissions of primary pollutants (those emitted directly from emission sources), although some secondary pollutants (those formed into the atmosphere from the reactions of primary ones), such as ammonium sulphate ( $(\text{NH}_4)_2\text{SO}_4$ ) also decreased.

Continuing decreasing current concentrations of AQ pollutants is a more complex target than before, because the need to decrease secondary pollutants, which is a difficult issue due to the non-linearity of many of their formation processes. Thus, to devise cost-effective AQ pollution measures a closer collaboration between the scientific

community (including European air quality and atmospheric science research communities, thematic European RIs, measurement harmonization bodies, such as AQUILA and national reference laboratories, data synthesis and integration providers, such as European Environmental Agency and data centers of the European RIs), AQ monitoring networks (AQMNs) and policy makers is needed. RI-URBANS focuses on this gap between science and policy to support developing an advanced AQ assessment to improve AQ in urban Europe.

To abate AQ pollutants there are important scientific, technological and policy challenges that vary according to the specific pollutant.

**Policy challenges:** An example is NO<sub>2</sub>. The abatement technologies and measures to be implemented to abate this pollutant are known and available. No need for further research or technology developments, it is a matter of implementation of policies with cost-effective technological and non-technological measures. Another policy challenge is that major AQ policy is developed at European level, but implementation (such as measurements and AQ plans) takes place at national level. EU bodies such as AQUILA, with the support of ESFRIs (e.g. ACTRIS) are basic to maintain a harmonised implementation of AQ measurements. However, the policy relevance given in the different EU-17 states to AQ issues varies widely and this should be also harmonised.

**Technology challenges:** For some sectors, technology development to abate emissions is still a challenge. Examples are i) developing and implementing technologies to burn domestic biomass without causing AQ impairments, and ii) idem for the emissions of volatile organic compounds (VOCs) in biomass-combustion based industrial and power plants.

**Scientific challenges:** Examples are i) the elaboration of cost-effective measures for abating secondary pollutants (such as O<sub>3</sub>, and 70% of PM<sub>2.5</sub> in urban background of European cities, Amato et al., 2016) in a scenario where O<sub>3</sub> and temperature increase due to climate change; and ii) abating secondary PM<sub>2.5</sub> under an urban increase of O<sub>3</sub> (that generate more oxidation of gaseous pollutants and, accordingly, more secondary PM).

There is a number of advanced AQ pollutants/parameters that might contribute to a cutting-edge AQ assessment for tackling the above AQ scientific challenges, and also, in some cases, to improve AQ monitoring for a better protection of human health and to support further reviews of AQ standards and parameters to be included in the future AQ legislation.

In the 2021 proposal, RI-URBANS suggested as advanced AQ parameters the measurement of ultrafine particles (UFP=nanoparticles), particle number size distribution (PNSD), black carbon (BC), PM speciation, oxidative potential (OP) of PM, VOCs and ammonia (NH<sub>3</sub>). These were included in the proposal for a new AQ Directive in October 2022, and moreover in the recently published new Directive on Ambient AQ for Europe (2024/2881/EC, NAQD).

RI-URBANS has produced [ST1](#) to [ST6](#) guidelines to help implement measurements on these advanced AQ pollutants/parameters. Furthermore, guidance on how to perform SA analyses of these pollutants/parameters is provided in [ST10](#) and [ST11](#). Also, the first emission EU inventory for UFP-PNSD, non-exhaust vehicle PM emissions, and guidance on improving multiscale emission inventories, and on multiscale modelling and assessing the impact of emission sources in criteria and novel pollutants, are provided by [ST15](#) and [ST16](#). All these STs will support an advanced AQ assessment based on an accurate SA of criteria and new pollutants, to identify causes of exceedances of the limit values, and to evaluate the effect of policy measures implemented and assess on future policies.

The measurement of novel AQ pollutants/parameters described in [ST1–ST6](#) shall be implemented at urban and rural AQ supersites in the EU, as outlined in Article 10 of the NAQD. AQUILA, the European network of National AQ Reference Laboratories, supports the implementation of existing EU air policy, and accordingly RI-URBANS and ACTRIS interacted with AQUILA and DG ENV from the European Commission for knowledge transfer and the co-design of the STs. It is also very important to connect these AQ monitoring efforts with those for urban greenhouse

gases, and, when possible, using the same supersites for both types of measurements in connection with the RI-URBANS twin project PAUL-ICOS-cities (<https://www.icos-cp.eu/projects/icos-cities>).

Furthermore, RI-URBANS also recommends implementing measurements of vertical profiles in [ST7-ST9](#), which are not recommended in the NAQD, but might provide essential data for AQ assessment, forecasting and management. These include the boundary layer dynamics (including mixing layer height, among others), the vertical aerosol profiles to detect external PM contributions, and the available IAGOS vertical profiles of pollutants measured in several European cities by using equipped commercial aircrafts. Furthermore, [ST12](#) and [ST13](#) provide guidance on the urban mapping and citizens involvement to obtain accurate spatial and time urban variations of pollution and increase awareness of the problem.

We have presented these STs in numerous stakeholders' meetings and discussed the contents of many of these with AQUILA, and in a number of cases produced them with ACTRIS. This document demonstrates how to access the guidance documents and provides examples of the added value generated by implementing these STs. We hope that the AQMNs and other AQ stakeholders will find these STs helpful in implementing the NAQD and further improving AQ across Europe.